Variational theory of superconductivity and application to the low-density electron gas

Yasutami Takada
Institute for Solid State Physics, University of Tokyo, Roppongi, Minato-ku, Tokyo 106, Japan
(Received 24 July 1987; revised manuscript received 9 October 1987)

The method of effective-potential expansion is employed to describe superconductivity in strongly correlated electron systems. We have obtained a gap equation in which both the pairing potential $V_p(\mathbf{k},\mathbf{k}')$ and the single-particle energy $\tilde{\varepsilon}_{\mathbf{k}}$ are expanded in terms of the effective potential. When the ring approximation or the random-phase approximation is used to evaluate each term in the expansion, $V_p(\mathbf{k},\mathbf{k}')$ and $\tilde{\varepsilon}_{\mathbf{k}}$ have the form $V_p^{\mathrm{KMK}}(\mathbf{k},\mathbf{k}')/z_{\mathbf{k}}z_{\mathbf{k}'}$, and $\varepsilon_{\mathbf{k}}^*/z_{\mathbf{k}}$, respectively, where V_p^{KMK} is the pairing potential derived by Kirzhnits, Maksimov, and Khomskii (KMK), $z_{\mathbf{k}}$ is the renormalization factor, and $\varepsilon_{\mathbf{k}}^*$ tends to the bare single-particle energy in the weak-coupling limit. Thus our theory may be viewed as an extension of the KMK theory to the strong-coupling region. The present general theory is applied to the electron gas in order to investigate whether the Coulomb interaction alone can cause superconductivity. We have improved on the two-body approximation to describe the normal state of the electron gas and have determined the effective potential variationally. With the use of the effective potential thus obtained, we have evaluated all terms up to second order for both $V_p(\mathbf{k},\mathbf{k}')$ and $\tilde{\varepsilon}_{\mathbf{k}}$. The pairing potential includes the plasmon-mediated attractive and the paramagnon-mediated repulsive parts as well as many complicated vertex corrections. We have solved the gap equation numerically and obtained the result that superconductivity appears at rather low carrier densities (i.e., $r_s > 3.9$). The highest transition temperature T_c in the range $30-60(m^*/\epsilon_0^2)$ K is obtained at $r_s \approx 7$, where m^* is the band mass in units of the free-electron mass and ϵ_0 is the dielectric constant. Our results might be useful to help explain the mechanism of superconductivity in the high-T_c oxide superconductors.

I. INTRODUCTION

At present, the most serious problem in the theory of calculating the superconducting transition temperature T_c from first principles is that we have only a little knowledge about the effect of electron-electron correlations on T_c.[1] The Coulomb effect is usually treated by the introduction of the Coulomb pseudopotential[2] μ^*. Ideally μ^* should be determined from an *ab initio* theory, but actually it is regarded as a phenomenological parameter. Furthermore, it is not yet known whether all the Coulomb effects can be pushed into a single parameter μ^* even in strongly correlated systems like heavy-fermion superconductors.[3]

Considerable progress in understanding the Coulomb effect on superconductivity will be made by a thorough investigation into the possibility of superconductivity in the electron gas without phonons. It is apparent that in the high-density limit, i.e., when the electronic density parameter r_s goes to zero, superconductivity does not appear in the system. However, in 1978 the present author[4] pointed out the possibility of superconductivity in the electron gas for $r_s > 6$ by treating the electron-electron interaction in the random-phase approximation (RPA) and evaluating T_c by the numerical solution of the gap equation in the weak-coupling Kirzhnitz, Maksimov, and Khomskii (KMK) scheme.[5] Later, Rietschel and Sham[6] showed that when the strong-coupling Eliashberg equation[7] was solved instead of the KMK scheme, the superconductivity was favored to appear even for $r_s > 2.5$. Thus we may conclude that the electron gas becomes superconducting in relatively low-electron-density systems, when the electron-electron interaction is treated in the RPA.

It is clear, however, that the RPA is not a good approximation for the electron gas having r_s larger than 1; we must consider the local-field correction. Grabowski and Sham[8] tried to go beyond the RPA, but their calculation was far from a first-principles one. Possibly, the ordinary Green's function method which they employed will not provide reliable results for this problem, because there are no good expansion parameters in the theory for the electron gas with $r_s > 1$. The coupled-cluster method[9] and the variational approach based on the hypernetted-chain approximation,[10] on the other hand, are known to give excellent results for the correlation energy ε_c in the range $1 \leqq r_s \leqq 20$.[11-13] There have been several attempts[14] to employ these methods to describe superconductivity, but none has made a detailed study of the electron gas yet. One of the problems in these approaches is that although ε_c is given quite accurately, the single-particle energy which we need to solve the gap equation is rather inaccurate.[12] Another problem is that it is not easy to relate the theory of superconductivity, thus obtained, with the well-developed conventional theory of superconductivity.[15,16]

The method of effective-potential expansion for the many-body problem[17] provides a very hopeful approach to the present problem. In this method, an effective potential $\tilde{V}$ is introduced to define a correlation operator which acts on the noninteracting ground state Φ_0 to create a many-body trial function $\tilde{\Phi}_0$. Any physical

quantity is expanded in terms of $\tilde{V}$, while $\tilde{V}$ itself is determined variationally. It has been shown previously,[18] that the normal properties of the electron gas can be described reasonably well even when we take a state described by a plane-wave Slater determinant for Φ_0 and neglect all terms higher than second order in $\tilde{V}$. (We denoted as the two-body approximation the cutoff of the cluster expansion at this level.) The relative error in ε_c compared to that obtained by the Green's-function Monte Carlo (GFMC) method[19] is less than 12% for $1 \leqq r_s \leqq 20$. In addition, virtually exact results for ε_c are obtained for $1 \leqq r_s \leqq 10$ when the ring and ring-exchange terms in third and fourth orders in $\tilde{V}$ are added to the terms in the two-body approximation.[20]

When we take the BCS state[21] for Φ_0, we obtain a theory of superconductivity in quite a straightforward way. A gap equation is obtained at $T=0$ for a gap $\Delta_{\mathbf{k}}$ of an electron with wave vector $\mathbf{k}$ as

$$\Delta_{\mathbf{k}} = -\sum_{\mathbf{k}'} V_p(\mathbf{k},\mathbf{k}')\Delta_{\mathbf{k}'}/2[\tilde{\varepsilon}_{\mathbf{k}'}^2+\Delta_{\mathbf{k}'}^2]^{1/2} . \tag{1.1}$$

Here, $V_p(\mathbf{k},\mathbf{k}')$ and $\tilde{\varepsilon}_{\mathbf{k}}$ are, respectively, the pairing potential and the single-particle energy, and are given in the power series of $\tilde{V}$ in which each term can be calculated with the help of the Feynman diagrams. We can relate these quantities easily with corresponding ones in the conventional theory of superconductivity. From such an analysis, it is seen that V_p and $\tilde{\varepsilon}_{\mathbf{k}}$ have the following structure:

$$V_p(\mathbf{k},\mathbf{k}') = V_p^*(\mathbf{k},\mathbf{k}')/z_{\mathbf{k}}z_{\mathbf{k}'} \tag{1.2}$$

and

$$\tilde{\varepsilon}_{\mathbf{k}} = \varepsilon_{\mathbf{k}}^*/z_{\mathbf{k}} , \tag{1.3}$$

where $z_{\mathbf{k}}$ is a so-called renormalization factor. Thus, despite its appearance, Eq. (1.1) is a gap equation for a strong-coupling superconductor. In addition, both V_p and $\tilde{\varepsilon}_{\mathbf{k}}$ can be expanded in terms of a square of the gap function:

$$V_p(\mathbf{k},\mathbf{k}') = V_p^{(0)}(\mathbf{k},\mathbf{k}') + \tfrac{1}{2}\sum_{\mathbf{pp}'} V_p^{(2)}(\mathbf{k},\mathbf{k}';\mathbf{p},\mathbf{p}')\Delta_{\mathbf{p}}\Delta_{\mathbf{p}'} + \cdots \tag{1.4}$$

and

$$\tilde{\varepsilon}_{\mathbf{k}} = \tilde{\varepsilon}_{\mathbf{k}}^{(0)} + \tfrac{1}{2}\sum_{\mathbf{pp}'} \tilde{\varepsilon}_{\mathbf{k}}^{(2)}(\mathbf{p},\mathbf{p}')\Delta_{\mathbf{p}}\Delta_{\mathbf{p}'} + \cdots . \tag{1.5}$$

Terms other than $V_p^{(0)}$ and $\tilde{\varepsilon}_{\mathbf{k}}^{(0)}$ describe the effect of fluctuations of Cooper pairs. Thus Eq. (1.1) goes beyond the mean-field theory. In this paper, however, we will neglect these fluctuation effects and evaluate V_p and $\tilde{\varepsilon}_{\mathbf{k}}$ in the normal limit, as has been done in the conventional theory of superconductivity. Strength of instability for superconductivity in Eq. (1.1) is measured by solving

$$\Delta_{\mathbf{k}} = -\sum_{\mathbf{k}'} V_p(\mathbf{k},\mathbf{k}')\frac{\Delta_{\mathbf{k}'}}{2\tilde{\varepsilon}_{\mathbf{k}'}}\tanh\left(\frac{\tilde{\varepsilon}_{\mathbf{k}'}}{2T_c}\right) . \tag{1.6}$$

We will call T_c thus obtained as the transition temperature in this paper.

As a first attempt to apply the present theory to the electron gas, we have tried to treat the problem as simply as possible. i.e., in the two-body approximation. However, it is found that the two-body approximation produces rather inaccurate results for V_p and $\tilde{\varepsilon}_{\mathbf{k}}$, in particular, near the Fermi surface. The problem is that the Coulomb potential cannot be screened completely by the sum of only a finite number of ring terms as is the case in the two-body approximation. In order to overcome this difficulty, the two-body approximation has been improved by the division of $\tilde{V}$ into long- and short-range parts, $\tilde{V}_l$ and $\tilde{V}_s$. All ring terms which are related with $\tilde{V}_l$ are summed up to infinite order, but we consider terms only up to second order in $\tilde{V}_s$ so as to make the calculations tractable. (Hereafter this approximation will be denoted as the modified two-body approximation.) As a result of this improvement, we have obtained ε_c whose relative error compared to the GFMC is reduced to 8% for $1 \leqq r_s \leqq 20$.

Even in the modified two-body approximation, we have found it very difficult at the present level of computer technology to evaluate all terms in V_p^* and $\varepsilon_{\mathbf{k}}^*$ without any approximation. Thus we have integrated ring-exchange, ladder, and ladder-exchange terms for V_p^* and $\varepsilon_{\mathbf{k}}^*$ in an approximate way. However, this approximation does not produce a serious error. For example, by calculating terms for $\varepsilon_{\mathbf{k}}^*$ at the Fermi level, we obtain the correlation part of the chemical potential μ_c. This can be compared with the value obtained by the GFMC, μ_c^{GFMC}, which is related to the correlation energy given by the GFMC, $\varepsilon_c^{\mathrm{GFMC}}$, through

$$\mu_c^{\mathrm{GFMC}} = \varepsilon_c^{\mathrm{GFMC}} - \frac{r_s}{3}\frac{\partial \varepsilon_c^{\mathrm{GFMC}}}{\partial r_s} . \tag{1.7}$$

We have found that the difference between μ_c and μ_c^{GFMC} is less than 7% for $1 \leqq r_s \leqq 10$, which is consistent with the difference between ε_c and $\varepsilon_c^{\mathrm{GFMC}}$. As for superconductivity, we have obtained the result that superconductivity appears in the electron gas for $r_s > 3.9$. As r_s is increased, T_c increases first, reaches its maximum at $r_s = 7.2$, and then decreases. The peak value for T_c is about 58 K $[m^*/(m_e\epsilon_0^2)]$, where m^*, m_e, and ϵ_0 are the band mass, the free-electron mass, and the dielectric constant, respectively.

In Sec. II, we give a basic formulation of the problem. We consider only ring terms in Sec. III and clarify the relation between the present theory and the conventional ones, especially the KMK theory. Section IV is devoted to the detailed account of the modified two-body approximation. Calculated results for ε_c and $z_{\mathbf{k}}^{-1}$ are given here. In Sec. V, we provide an expression for V_p^* and $\varepsilon_{\mathbf{k}}^*$ and show numerical results for μ_c, $\tilde{\varepsilon}_{\mathbf{k}}$, V_p, $\Delta_{\mathbf{k}}$, and T_c.[22] The present study may provide useful information about the mechanism of high-T_c superconductivity in La-Sr-Cu-O and Y-Ba-Cu-O,[23] although at present we admit that the electron gas is not proven to be a good model for these systems. We discuss this problem in Sec. VI, together with other related problems.

II. VARIATIONAL STATE FOR SUPERCONDUCTIVITY

A. Bogoliubov transformation

The Hamiltonian for the electron gas in a uniform positive background is written, in second quantization, as

$$H=\sum_{\mathbf{k}\sigma}\varepsilon_{\mathbf{k}}C^{\dagger}_{\mathbf{k}\sigma}C_{\mathbf{k}\sigma}+\tfrac{1}{2}\sum_{\mathbf{q}\neq 0}\sum_{\mathbf{k}\sigma}\sum_{\mathbf{k}'\sigma'}V(q)C^{\dagger}_{\mathbf{k}+\mathbf{q}\sigma}C^{\dagger}_{\mathbf{k}'-\mathbf{q}\sigma'}C_{\mathbf{k}'\sigma'}C_{\mathbf{k}\sigma}\ , \tag{2.1}$$

with $\varepsilon_{\mathbf{k}}=\mathbf{k}^2/2m^*$ and $V(q)=4\pi e^2/\epsilon_0 q^2$. As usual, $\hbar$ is taken to be unity, $C_{\mathbf{k}\sigma}$ is the destruction operator of an electron specified by wave vector $\mathbf{k}$ and spin σ. The Bogoliubov transformation[24] S is defined by

$$\alpha_{\mathbf{k}\uparrow}=u_{\mathbf{k}}C_{\mathbf{k}\uparrow}-v_{\mathbf{k}}C^{\dagger}_{-\mathbf{k}\downarrow} \tag{2.2a}$$

and

$$\alpha_{-\mathbf{k}\downarrow}=u_{\mathbf{k}}C_{-\mathbf{k}\downarrow}+v_{\mathbf{k}}C^{\dagger}_{\mathbf{k}\uparrow}\ , \tag{2.2b}$$

where $u_{\mathbf{k}}$ and $v_{\mathbf{k}}$ satisfy the relations

$$u^2_{\mathbf{k}}+v^2_{\mathbf{k}}=1\ , \tag{2.3}$$

$$u_{\mathbf{k}}=u_{-\mathbf{k}}\ , \tag{2.4a}$$

and

$$v_{\mathbf{k}}=v_{-\mathbf{k}}\ . \tag{2.4b}$$

When we apply the transformation S to the operator of the thermodynamic potential at $T=0$, we obtain

$$\Omega\equiv S^{-1}(H-\mu N)S=\Omega_0+\Omega_2+\Omega_4\ , \tag{2.5}$$

where μ is the chemical potential, Ω_0, Ω_2, and Ω_4 are given, respectively, as

$$\Omega_0=\sum_{\mathbf{k}}2(\varepsilon_{\mathbf{k}}-\mu)v^2_{\mathbf{k}}-\sum_{\mathbf{k}}\sum_{\mathbf{k}'(\neq\mathbf{k})}V(\mathbf{k}-\mathbf{k}')v^2_{\mathbf{k}}v^2_{\mathbf{k}'}+\sum_{\mathbf{q}\neq 0}\sum_{\mathbf{k}}V(q)u_{\mathbf{k}+\mathbf{q}}v_{\mathbf{k}+\mathbf{q}}u_{\mathbf{k}}v_{\mathbf{k}}\ , \tag{2.6}$$

$$\Omega_2=\sum_{\mathbf{k}}E_{\mathbf{k}}(\alpha^{\dagger}_{\mathbf{k}\uparrow}\alpha_{\mathbf{k}\uparrow}+\alpha^{\dagger}_{-\mathbf{k}\downarrow}\alpha_{-\mathbf{k}\downarrow})+\sum_{\mathbf{k}}D_{\mathbf{k}}(\alpha^{\dagger}_{\mathbf{k}\uparrow}\alpha^{\dagger}_{-\mathbf{k}\downarrow}+\alpha_{-\mathbf{k}\downarrow}\alpha_{\mathbf{k}\uparrow})\ , \tag{2.7}$$

and

$$\begin{aligned}\Omega_4=&\tfrac{1}{2}\sum_{\mathbf{q}\neq 0}\sum_{\mathbf{k}\sigma}\sum_{\mathbf{k}'\sigma'}V(q)\Gamma_{\mathbf{k}+\mathbf{q},\mathbf{k}}\Gamma_{\mathbf{k}'+\mathbf{q},\mathbf{k}'}\alpha^{\dagger}_{\mathbf{k}+\mathbf{q}\sigma}\alpha^{\dagger}_{-\mathbf{k}'-\mathbf{q}\sigma'}\alpha_{-\mathbf{k}'\sigma'}\alpha_{\mathbf{k}\sigma}+\sum_{\mathbf{q}\neq 0}\sum_{\mathbf{k}}\sum_{\mathbf{k}'}V(q)\tilde{\Gamma}_{\mathbf{k}+\mathbf{q},\mathbf{k}}\tilde{\Gamma}_{\mathbf{k}'+\mathbf{q},\mathbf{k}'}\alpha^{\dagger}_{\mathbf{k}+\mathbf{q}\uparrow}\alpha^{\dagger}_{-\mathbf{k}\downarrow}\alpha_{-\mathbf{k}'\downarrow}\alpha_{\mathbf{k}'+\mathbf{q}\uparrow}\\&+\tfrac{1}{2}\sum_{\mathbf{q}\neq 0}\sum_{\mathbf{k}}\sum_{\mathbf{k}'}V(q)\tilde{\Gamma}_{\mathbf{k}+\mathbf{q},\mathbf{k}}\tilde{\Gamma}_{\mathbf{k}'+\mathbf{q},\mathbf{k}'}(\alpha^{\dagger}_{\mathbf{k}+\mathbf{q}\uparrow}\alpha^{\dagger}_{-\mathbf{k}\downarrow}\alpha^{\dagger}_{-\mathbf{k}'-\mathbf{q}\uparrow}\alpha^{\dagger}_{\mathbf{k}'\downarrow}+\text{c.c.})\\&+\sum_{\mathbf{q}\neq 0}\sum_{\mathbf{k}}\sum_{\mathbf{k}'\sigma'}V(q)\tilde{\Gamma}_{\mathbf{k}+\mathbf{q},\mathbf{k}}\Gamma_{\mathbf{k}'+\mathbf{q},\mathbf{k}'}(\alpha^{\dagger}_{\mathbf{k}+\mathbf{q}\uparrow}\alpha^{\dagger}_{-\mathbf{k}\downarrow}\alpha^{\dagger}_{-\mathbf{k}'-\mathbf{q}\sigma'}\alpha_{-\mathbf{k}'\sigma'}+\text{c.c})\ ,\end{aligned} \tag{2.8}$$

with

$$E_{\mathbf{k}}=\left[\varepsilon_{\mathbf{k}}-\mu-\sum_{\mathbf{k}'\neq\mathbf{k}}V(\mathbf{k}-\mathbf{k}')v^2_{\mathbf{k}'}\right](u^2_{\mathbf{k}}-v^2_{\mathbf{k}})-2\sum_{\mathbf{q}\neq 0}V(q)u_{\mathbf{k}+\mathbf{q}}v_{\mathbf{k}+\mathbf{q}}u_{\mathbf{k}}v_{\mathbf{k}}\ , \tag{2.9}$$

$$D_{\mathbf{k}}=2\left[\varepsilon_{\mathbf{k}}-\mu-\sum_{\mathbf{k}'\neq\mathbf{k}}V(\mathbf{k}-\mathbf{k}')v^2_{\mathbf{k}'}\right]u_{\mathbf{k}}v_{\mathbf{k}}+\sum_{\mathbf{q}\neq 0}V(q)u_{\mathbf{k}+\mathbf{q}}v_{\mathbf{k}+\mathbf{q}}(u^2_{\mathbf{k}}-v^2_{\mathbf{k}})\ , \tag{2.10}$$

$$\Gamma_{\mathbf{k}+\mathbf{q},\mathbf{k}}=u_{\mathbf{k}+\mathbf{q}}u_{\mathbf{k}}-v_{\mathbf{k}+\mathbf{q}}v_{\mathbf{k}}\ , \tag{2.11}$$

and

$$\tilde{\Gamma}_{\mathbf{k}+\mathbf{q},\mathbf{k}}=u_{\mathbf{k}+\mathbf{q}}v_{\mathbf{k}}+u_{\mathbf{k}}v_{\mathbf{k}+\mathbf{q}}\ . \tag{2.12}$$

B. Trial function

For the ground-state wave function, we consider the following trial function:[17]

$$|\tilde{\Phi}_0\rangle=\sum_{n=0}^{\infty}\frac{1}{n!}\left[\sum_{m=1}^{\infty}U_m(0,-\infty)\right]^n|\Phi_0\rangle\ , \tag{2.13}$$

where Φ_0 is the vacuum state of $\alpha_{\mathbf{k}\sigma}$, i.e.,

$$\alpha_{\mathbf{k}\sigma}|\Phi_0\rangle=0\ , \tag{2.14}$$

and the correlation operator, U_m, is defined with the use of the long- and short-range parts of the effective potential, $\tilde{V}_l$ and $\tilde{V}_s$, as

$$U_m(0,-\infty)=\frac{(-i)^m}{m!}\int_{-\infty}^{0}e^{0^+t_1}dt_1\cdots\int_{-\infty}^{0}e^{0^+t_m}dt_m\,T[\tilde{V}_l(t_1)\cdots\tilde{V}_l(t_m)]_L$$
$$+\frac{(-i)^m}{(m-1)!}\int_{-\infty}^{0}e^{0^+t_1}dt_1\cdots\int_{-\infty}^{0}e^{0^+t_m}dt_m\,T[\tilde{V}_s(t_1)\tilde{V}_l(t_2)\cdots\tilde{V}_l(t_m)]_L\ . \quad (2.15)$$

Here, $\tilde{V}_l(t)$ and $\tilde{V}_s(t)$ are, respectively, defined as

$$\tilde{V}_l(t)=\exp(i\tilde{H}_0t)\tilde{V}_l\exp(-i\tilde{H}_0t) \quad (2.16a)$$

and

$$\tilde{V}_s(t)=\exp(i\tilde{H}_0t)\tilde{V}_s\exp(-i\tilde{H}_0t)\ , \quad (2.16b)$$

with some suitably chosen noninteracting Hamiltonian $\tilde{H}_0$. The symbol T and the subscript L represent, respectively, the T product and the instruction to collect only terms described by linked graphs. [It should be noted that each cluster enclosed by the T operator does not link directly to other clusters in the definition of Eq. (2.13), as in previous publication.[17,18,20]] In this paper, we choose the following forms for $\tilde{H}_0$, $\tilde{V}_l$, and $\tilde{V}_s$:

$$\tilde{H}_0=\sum_{\mathbf{k}}e_{\mathbf{k}}(\alpha^\dagger_{\mathbf{k}\uparrow}\alpha_{\mathbf{k}\uparrow}+\alpha^\dagger_{-\mathbf{k}\downarrow}\alpha_{-\mathbf{k}\downarrow})\ , \quad (2.17)$$

$$\tilde{V}_l=\tfrac{1}{2}\sum_{\mathbf{q}\neq0}\sum_{\mathbf{k}\mathbf{k}'}\tilde{V}_l(q)\tilde{\Gamma}_{\mathbf{k}+\mathbf{q},\mathbf{k}}\tilde{\Gamma}_{\mathbf{k}'+\mathbf{q},\mathbf{k}'}$$
$$\times(\alpha^\dagger_{\mathbf{k}+\mathbf{q}\uparrow}\alpha^\dagger_{-\mathbf{k}\downarrow}\alpha^\dagger_{-\mathbf{k}'-\mathbf{q}\uparrow}\alpha^\dagger_{\mathbf{k}'\downarrow}+\text{c.c.})$$
$$+\sum_{\mathbf{q}\neq0}\sum_{\mathbf{k}\mathbf{k}'}\tilde{V}_l(q)\tilde{\Gamma}_{\mathbf{k}+\mathbf{q},\mathbf{k}}\tilde{\Gamma}_{\mathbf{k}'+\mathbf{q},\mathbf{k}'}\alpha^\dagger_{\mathbf{k}+\mathbf{q}\uparrow}\alpha^\dagger_{-\mathbf{k}\downarrow}\alpha_{-\mathbf{k}'\downarrow}\alpha_{\mathbf{k}'+\mathbf{q}\uparrow}\ , \quad (2.18)$$

and

$$\tilde{V}_s=\tfrac{1}{2}\sum_{\mathbf{q}\neq0}\sum_{\mathbf{k}\mathbf{k}'}\tilde{V}_s(q)\tilde{\Gamma}_{\mathbf{k}+\mathbf{q},\mathbf{k}}\tilde{\Gamma}_{\mathbf{k}'+\mathbf{q},\mathbf{k}'}$$
$$\times(\alpha^\dagger_{\mathbf{k}+\mathbf{q}\uparrow}\alpha^\dagger_{-k\downarrow}\alpha^\dagger_{-\mathbf{k}'-\mathbf{q}\uparrow}\alpha^\dagger_{\mathbf{k}'\downarrow}+\text{c.c})\ , \quad (2.19)$$

where $e_{\mathbf{k}}$ is defined by

$$e_{\mathbf{k}}=|\,\varepsilon_{\mathbf{k}}-\mu_H\,|\ , \quad (2.20)$$

with the use of the Hartree part of the chemical potential $\mu_H\equiv k_F^2/2m^*$ in which k_F is the Fermi wave vector. The effective potentials $\tilde{V}_l(q)$ and $\tilde{V}_s(q)$ will be determined variationally, but we assume that $\tilde{V}_l(q)$ becomes negligibly small for q larger than $0.1k_F$.

C. Energy expectation value

The expectation value for the thermodynamic potential $\langle\Omega\rangle$ with respect to $|\tilde{\Phi}_0\rangle$ can be calculated with the use of the linked-cluster theorem, as shown in Ref. 17. We will write $\langle\Omega\rangle$ in power series of $\tilde{V}_s$ as

$$\langle\Omega\rangle\equiv\langle\tilde{\Phi}_0|\,\Omega\,|\tilde{\Phi}_0\rangle/\langle\tilde{\Phi}_0|\tilde{\Phi}_0\rangle=\sum_{n=0}^{\infty}\Omega^{(n)}\ . \quad (2.21)$$

Here, $\Omega^{(n)}$ is the nth-order term in $\tilde{V}_s$, but it can still be expanded in $\tilde{V}_l$ up to infinite order. On the assumption that $\tilde{V}_l(q)$ vanishes except for very small q, an important contribution will come only from ring terms in the expansion. As a result, we obtain an expression for $\langle\Omega\rangle$ which is almost the same as in Refs. 18 and 20. The only difference is that the effective potential $\tilde{V}$ in these references is replaced by $\tilde{V}_s$ with some appropriate screening factor induced by the sum of ring terms in $\tilde{V}_l$. We can sum these ring terms up to infinite order by the same procedure Gell-Mann and Brueckner[25] used in 1957.

III. SUPERCONDUCTIVITY IN THE RING APPROXIMATION

A. Total energy

Before we try to solve the full problem described in Sec. II, we consider the problem in the ring approximation. For the purpose, we may take $\tilde{V}_s(q)$ to be zero and calculate $\Omega^{(0)}$ by taking only ring diagrams into account [we will not assume that $\tilde{V}_l(q)$ becomes negligibly small for large q in this section].

In accordance with the division of Ω in Eq. (2.5), there are three contributions to $\Omega^{(0)}$. The first one is Ω_0 itself and others come from $\langle\Omega_2\rangle$ and $\langle\Omega_4\rangle$. Let us consider $\langle\Omega_4\rangle$ first. First-order terms in $\tilde{V}_l$ are given in Fig. 1(a) in the Goldstone diagram and can be described as

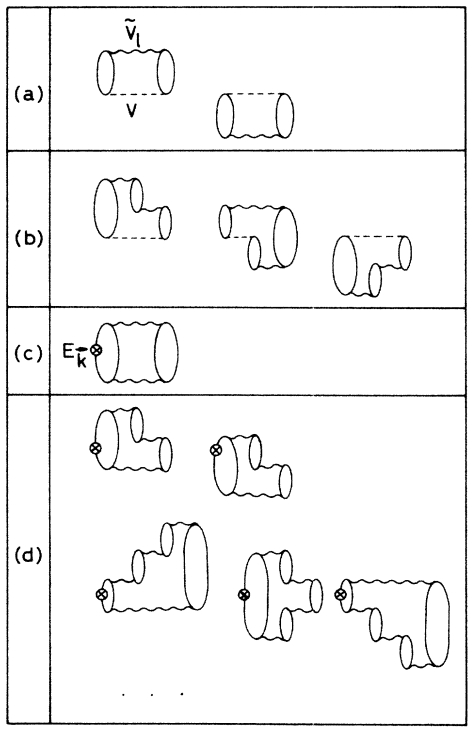

FIG. 1. Goldstone diagrams for $\Omega^{(0)}$.

$$C^{(0)}_{1,0}(\Omega_4)+C^{(0)}_{0,1}(\Omega_4)=-\sum_{\mathbf{q}\neq 0}\sum_{\mathbf{k}\mathbf{k}'} V(q)\tilde{V}_l(q)\tilde{\Gamma}^2_{\mathbf{k}+\mathbf{q},\mathbf{k}}\tilde{\Gamma}^2_{\mathbf{k}'+\mathbf{q},\mathbf{k}'}/(e_{\mathbf{k}}+e_{\mathbf{k}+\mathbf{q}}+e_{\mathbf{k}'}+e_{\mathbf{k}'+\mathbf{q}}) . \tag{3.1}$$

By introducing the polarization function, $\Pi(q,\omega)$, defined by

$$\Pi(q,\omega)=\sum_{\mathbf{k}}\int\frac{d\omega'}{2\pi i}\tilde{\Gamma}^2_{\mathbf{k}+\mathbf{q},\mathbf{k}}\left[\frac{1}{-\omega'+i0^+-e_{\mathbf{k}}}\frac{1}{\omega+\omega'+i0^+-e_{\mathbf{k}+\mathbf{q}}}+\frac{1}{\omega'+i0^+-e_{\mathbf{k}}}\frac{1}{-\omega-\omega'+i0^+-e_{\mathbf{k}+\mathbf{q}}}\right]$$

$$=\sum_{\mathbf{k}}\tilde{\Gamma}^2_{\mathbf{k}+\mathbf{q},\mathbf{k}}\left[\frac{1}{\omega-i0^+ +e_{\mathbf{k}}+e_{\mathbf{k}+\mathbf{q}}}-\frac{1}{\omega+i0^+ -e_{\mathbf{k}}-e_{\mathbf{k}+\mathbf{q}}}\right], \tag{3.2}$$

we can rewrite Eq. (3.1) as

$$C^{(0)}_{1,0}(\Omega_4)+C^{(0)}_{0,1}(\Omega_4)=-\tfrac{1}{2}\sum_{\mathbf{q}\neq 0}\int\frac{d\omega}{2\pi i}V(q)\tilde{V}_l(q)\Pi(q,\omega)^2 . \tag{3.3}$$

Second-order terms are composed of three diagrams in Fig. 1(b). We can sum these terms to get

$$C^{(0)}_{2,0}(\Omega_4)+C^{(0)}_{1,1}(\Omega_4)+C^{(0)}_{0,2}(\Omega_4)=\tfrac{1}{2}\sum_{\mathbf{q}\neq 0}\int\frac{d\omega}{2\pi i}V(q)\tilde{V}_l(q)^2\Pi(q,\omega)^3 . \tag{3.4}$$

Higher-order terms are also written in a similar way. By summing all these terms, we obtain

$$\langle\Omega_4\rangle=-\tfrac{1}{2}\sum_{\mathbf{q}\neq 0}\int\frac{d\omega}{2\pi i}V(q)\tilde{V}_l(q)\Pi(q,\omega)^2/[1+\tilde{V}_l(q)\Pi(q,\omega)] . \tag{3.5}$$

Now, we will calculate $\langle\Omega_2\rangle$. It is easily seen that terms connected with $D_{\mathbf{k}}$ in Eq. (2.7) always vanish for the trial function in Eq. (2.13) with $\tilde{V}_l$ and $\tilde{V}_s$ in Eqs. (2.18) and (2.19). The first nonvanishing contribution to $\langle\Omega_2\rangle$ is given in Fig. 1(c) and written as

$$C^{(0)}_{1,1}(\Omega_2)=\tfrac{1}{2}\sum_{\mathbf{q}\neq 0}\sum_{\mathbf{k}\mathbf{k}'}\tilde{V}_l(q)^2\tilde{\Gamma}^2_{\mathbf{k}+\mathbf{q},\mathbf{k}}\tilde{\Gamma}^2_{\mathbf{k}'+\mathbf{q},\mathbf{k}'}(E_{\mathbf{k}}+E_{\mathbf{k}+\mathbf{q}}+E_{\mathbf{k}'}+E_{\mathbf{k}'+\mathbf{q}})/(e_{\mathbf{k}}+e_{\mathbf{k}+\mathbf{q}}+e_{\mathbf{k}'}+e_{\mathbf{k}'+\mathbf{q}})^2$$

$$=\sum_{\mathbf{q}\neq 0}\int\frac{d\omega}{2\pi i}\tilde{V}_l(q)^2\Pi(q,\omega)\sum_{\mathbf{k}}\tilde{\Gamma}^2_{\mathbf{k}+\mathbf{q},\mathbf{k}}E_{\mathbf{k}}\left[\frac{1}{(\omega-i0^+ +e_{\mathbf{k}}+e_{\mathbf{k}+\mathbf{q}})^2}+\frac{1}{(\omega+i0^+ -e_{\mathbf{k}}-e_{\mathbf{k}+\mathbf{q}})^2}\right] . \tag{3.6}$$

By considering higher-order terms in Fig. 1(d), we obtain

$$\langle\Omega_2\rangle=-\sum_{\mathbf{q}\neq 0}\int\frac{d\omega}{2\pi i}\frac{\tilde{V}_l(q)}{1+\tilde{V}_l(q)\Pi(q,\omega)}\sum_{\mathbf{k}}\tilde{\Gamma}^2_{\mathbf{k}+\mathbf{q},\mathbf{k}}E_{\mathbf{k}}\left[\frac{1}{(\omega-i0^+ +e_{\mathbf{k}}+e_{\mathbf{k}+\mathbf{q}})^2}+\frac{1}{(\omega+i0^+ -e_{\mathbf{k}}-e_{\mathbf{k}+\mathbf{q}})^2}\right] . \tag{3.7}$$

In the ring approximation, $E_{\mathbf{k}}$ in Eqs. (3.6) and (3.7) should not be the form in Eq. (2.9) but rather

$$E_{\mathbf{k}}=(\varepsilon_{\mathbf{k}}-\mu_H)\cdot(u^2_{\mathbf{k}}-v^2_{\mathbf{k}})-2\sum_{\mathbf{q}\neq 0}V(q)u_{\mathbf{k}+\mathbf{q}}v_{\mathbf{k}+\mathbf{q}}u_{\mathbf{k}}v_{\mathbf{k}} . \tag{3.8}$$

(The Fock term in $E_{\mathbf{k}}$ produces the self-energy diagram in the notation of Refs. 18 and 20 and should be neglected.)

B. Determination of $\tilde{V}_l(q)$

We can obtain $\Omega^{(0)}$ by the sum of Ω_0 in Eq. (2.6), $\langle\Omega_4\rangle$ in Eq. (3.5), and $\langle\Omega_2\rangle$ in Eq. (3.7) with $E_{\mathbf{k}}$ in Eq. (3.8). In the normal limit, i.e., $v^2_{\mathbf{k}}=n_{\mathbf{k}}$ and $u^2_{\mathbf{k}}=1-n_{\mathbf{k}}$ with

$$n_{\mathbf{k}}=\begin{cases}1 & \text{for } |\mathbf{k}|<k_F\\ 0 & \text{for } |\mathbf{k}|>k_F,\end{cases} \tag{3.9}$$

$\Omega^{(0)}$ is rewritten as

$$\Omega^{(0)}=\sum_{\mathbf{k}}2(\varepsilon_k-\mu)n_{\mathbf{k}}-\sum_{\mathbf{k}}\sum_{\mathbf{k}'(\neq\mathbf{k})}V(\mathbf{k}-\mathbf{k}')n_{\mathbf{k}}n_{\mathbf{k}'}+\tfrac{1}{2}\sum_{\mathbf{q}\neq 0}\int_0^\infty\frac{d\omega}{\pi}\left[\ln[1+\tilde{V}_l\Pi_0(q,i\omega)]\right.$$

$$\left.-\tilde{V}_l(q)\Pi_0(q,i\omega)\frac{1+V(q)\Pi_0(q,i\omega)}{1+\tilde{V}_l(q)\Pi_0(q,i\omega)}\right], \tag{3.10}$$

where the polarization function for the imaginary frequency $i\omega$ in the normal limit $\Pi_0(q,i\omega)$ is given by

$$\Pi_0(q,i\omega)=\sum_{\mathbf{k}\sigma}n_{\mathbf{k}}(1-n_{\mathbf{k}+\mathbf{q}})(\varepsilon_{\mathbf{k}+\mathbf{q}}-\varepsilon_{\mathbf{k}})/[\omega^2+(\varepsilon_{\mathbf{k}+\mathbf{q}}-\varepsilon_{\mathbf{k}})^2] . \tag{3.11}$$

In deriving Eq. (3.10), we have used the identity

$$\sum_{\mathbf{k}\sigma} n_{\mathbf{k}}(1-n_{\mathbf{k}+\mathbf{q}})(\varepsilon_{\mathbf{k}+\mathbf{q}}-\varepsilon_{\mathbf{k}})[(\varepsilon_{\mathbf{k}+\mathbf{q}}-\varepsilon_{\mathbf{k}})^2-\omega^2]/[(\varepsilon_{\mathbf{k}+\mathbf{q}}-\varepsilon_{\mathbf{k}})^2+\omega^2]^2=\frac{\omega}{2}\frac{\partial\Pi_0(q,i\omega)}{\partial\omega}+\tfrac{1}{2}\Pi_0(q,i\omega)\ , \tag{3.12}$$

and performed an integral by parts to obtain a ln term.

When we take a functional derivative of Eq. (3.10) with respect to $V_l(q)$, we get

$$\frac{\delta\Omega^{(0)}}{\delta\tilde{V}_l(q)}=\tfrac{1}{2}\int_0^\infty\frac{d\omega}{\pi}\frac{\Pi_0(q,i\omega)^2}{[1+\tilde{V}_l(q)\Pi_0(q,i\omega)]^2}[\tilde{V}_l(q)-V(q)]\ . \tag{3.13}$$

Thus, in the ring approximation, $\Omega^{(0)}$ is minimized when $\tilde{V}_l(q)$ is taken to be $V(q)$. By substituting $V(q)$ for $\tilde{V}_l(q)$ in Eq. (3.10), we have an expression for the total energy which is just the same as that in the RPA in the ordinary Green's-function method.[25–28]

C. Gap equation

For a given $\tilde{V}_l(q)$, a gap equation can be obtained by the optimization condition for $v_{\mathbf{k}}$, i.e., $\delta\Omega^{(0)}/\delta v_{\mathbf{k}}=0$. We can express it in the form

$$2\tilde{\varepsilon}_{\mathbf{k}}u_{\mathbf{k}}v_{\mathbf{k}}=-\sum_{\mathbf{k}'}V_p(\mathbf{k},\mathbf{k}')u_{\mathbf{k}'}v_{\mathbf{k}'}(u_{\mathbf{k}}^2-v_{\mathbf{k}}^2)\ , \tag{3.14}$$

where in the normal limit, the single-particle energy $\tilde{\varepsilon}_{\mathbf{k}}$ and the pairing potential $V_p(\mathbf{k},\mathbf{k}')$ are given, respectively, as

$$\tilde{\varepsilon}_{\mathbf{k}}=\varepsilon_{\mathbf{k}}^*+(\varepsilon_{\mathbf{k}}-\mu_H)\Delta z_{\mathbf{k}} \tag{3.15}$$

and

$$V_p(\mathbf{k},\mathbf{k}')=V_p^*(\mathbf{k},\mathbf{k}')+V(q)(\Delta z_{\mathbf{k}}+\Delta z_{\mathbf{k}'})\ , \tag{3.16}$$

with

$$\varepsilon_{\mathbf{k}}^*=\varepsilon_{\mathbf{k}}-\mu-\sum_{\mathbf{k}'\neq\mathbf{k}}V(\mathbf{k}-\mathbf{k}')n_{\mathbf{k}'}+\sum_{\mathbf{q}\neq0}\int_0^\infty\frac{d\omega}{\pi}\left[\frac{V(q)+\tilde{V}_l(q)^2\Pi_0(q,i\omega)}{[1+\tilde{V}_l(q)\Pi_0(q,i\omega)]^2}-V(q)\right]$$
$$\times(1-2n_{\mathbf{k}+\mathbf{q}})(e_{\mathbf{k}}+e_{\mathbf{k}+\mathbf{q}})/[\omega^2+(e_{\mathbf{k}}+e_{\mathbf{k}+\mathbf{q}})^2]\ , \tag{3.17}$$

$$V_p^*(\mathbf{k},\mathbf{k}'\equiv\mathbf{k}+\mathbf{q})=V(q)+\int_0^\infty\frac{2}{\pi}d\omega\left[\frac{V(q)+\tilde{V}_l(q)^2\Pi_0(q,i\omega)}{[1+\tilde{V}_l(q)\Pi_0(q,i\omega)]^2}-V(q)\right](e_{\mathbf{k}}+e_{\mathbf{k}+\mathbf{q}})/[\omega^2+(e_{\mathbf{k}}+e_{\mathbf{k}+\mathbf{q}})^2]\ , \tag{3.18}$$

and

$$\Delta z_{\mathbf{k}}=\sum_{\mathbf{q}\neq0}\int_0^\infty\frac{2}{\pi}d\omega\frac{\tilde{V}_l(q)}{1+\tilde{V}_l(q)\Pi_0(q,i\omega)}[n_{\mathbf{k}}(1-n_{\mathbf{k}+\mathbf{q}})+n_{\mathbf{k}+\mathbf{q}}(1-n_{\mathbf{k}})][(e_{\mathbf{k}}+e_{\mathbf{k}+q})^2-\omega^2]/[\omega^2+(e_{\mathbf{k}}+e_{\mathbf{k}+q})^2]^2\ . \tag{3.19}$$

When we introduce the gap function $\Delta_{\mathbf{k}}$ by

$$\Delta_{\mathbf{k}}=-\sum_{\mathbf{k}'}V_p(\mathbf{k},\mathbf{k}')u_{\mathbf{k}'}v_{\mathbf{k}'}\ , \tag{3.20}$$

and solve Eq. (3.14) in terms of $\Delta_{\mathbf{k}}$ as

$$u_{\mathbf{k}}^2=[1+\tilde{\varepsilon}_{\mathbf{k}}/(\tilde{\varepsilon}_{\mathbf{k}}^2+\Delta_{\mathbf{k}}^2)^{1/2}]/2 \tag{3.21a}$$

and

$$v_{\mathbf{k}}^2=[1-\tilde{\varepsilon}_{\mathbf{k}}/(\tilde{\varepsilon}_{\mathbf{k}}^2+\Delta_{\mathbf{k}}^2)^{1/2}]/2\ , \tag{3.21b}$$

we can change Eq. (3.14) into the form Eq. (1.1).

The second terms in Eqs. (3.15) and (3.16) arise from the derivative of $E_{\mathbf{k}}$ given in Eq. (3.8) with respect to $v_{\mathbf{k}}$. These terms correspond to the renormalization of the bare single-particle state. Although we have expressions for $\tilde{\varepsilon}_{\mathbf{k}}$ and V_p in Eqs. (3.15) and (3.16), in which this renormalization effect has been included only for the bare single-particle energy $\varepsilon_{\mathbf{k}}-\mu_H$ and the bare potential $V(q)$, it is physically more reasonable to include this effect even for other parts of the single-particle energy and the pairing potential by the redefinition of $\tilde{\varepsilon}_{\mathbf{k}}$ and V_p in the form of Eqs. (1.2) and (1.3), where ε_k^* and V_p^* have already been given in Eqs. (3.17) and (3.18), respectively, and the renormalization factor $z_{\mathbf{k}}^{-1}$ is defined by

$$z_{\mathbf{k}}^{-1}=1+\Delta z_{\mathbf{k}}\ , \tag{3.22}$$

with $\Delta z_{\mathbf{k}}$ given in Eq. (3.19). In the present approximation, z_k^{-1} is related to the occupation number in the normal state, $N_k\equiv\langle C_{\mathbf{k}\sigma}^\dagger C_{\mathbf{k}\sigma}\rangle$, through

$$N_k=\begin{cases}\frac{1}{2}(1+z_{\mathbf{k}}^{-1}) & \text{for } |\mathbf{k}|<k_F,\\ \frac{1}{2}(1-z_{\mathbf{k}}^{-1}) & \text{for } |\mathbf{k}|>k_F.\end{cases} \tag{3.23}$$

At the Fermi surface, there is a discontinuity in N_k, as well as in $z_{\mathbf{k}}^{-1}$, but the magnitude of the discontinuity in the occupation number is equal to the average of $z_{k_F-0^+}^{-1}$ and $z_{k_F+0^+}^{-1}$ which defines the renormalization factor at the Fermi surface $z_{k_F}^{-1}$:

$$z_{k_F}^{-1}=\tfrac{1}{2}(z_{k_F-0^+}^{-1}+z_{k_F+0^+}^{-1}) . \tag{3.24}$$

When $\tilde{V}_l(q)$ is small, to make $\Delta z_{\mathbf{k}}$ defined in Eq. (3.19) also small, it does not matter whether we use Eqs. (3.15) and (3.16) for $\tilde{\varepsilon}_{\mathbf{k}}$ and $V_p(\mathbf{k},\mathbf{k}')$ or Eqs. (1.2) and (1.3). In the ring approximation, however, $\tilde{V}_l(q)$ is equal to $V(q)$ and is not small. Thus, the physical quantities like T_c depend on the choice of equations for $\tilde{\varepsilon}_{\mathbf{k}}$ and $V_p(\mathbf{k},\mathbf{k}')$. We will see how much T_c changes with the choices of (a) Eqs. (1.2) and (1.3), (b) Eqs. (3.15) and (3.16), and (c) $\varepsilon_{\mathbf{k}}-\mu_H$ and $V_p^*(\mathbf{k},\mathbf{k}')$ for $\tilde{\varepsilon}_{\mathbf{k}}$ and $V_p(\mathbf{k},\mathbf{k}')$. In general, choice (a) gives the lowest T_c.

D. Relation with the KMK theory

When we substitute $V(q)$ for $\tilde{V}_l(q)$, we can rewrite Eq. (3.18) as

$$\begin{aligned}V_p^*(\mathbf{k},\mathbf{k}'\equiv\mathbf{k}+\mathbf{q})&=\int_0^\infty\frac{2}{\pi}d\omega\frac{V(q)}{1+V(q)\Pi_0(q,i\omega)}\frac{e_{\mathbf{k}}+e_{\mathbf{k}+\mathbf{q}}}{\omega^2+(e_{\mathbf{k}}+e_{\mathbf{k}+\mathbf{q}})^2}\\&=V(q)\left[1+2\int_0^\infty\frac{d\omega}{\pi}\mathrm{Im}\left[\frac{1}{1+V(q)\Pi_0(q,\omega)}\right]\frac{1}{\omega+e_{\mathbf{k}}+e_{\mathbf{k}+q}}\right] .\end{aligned} \tag{3.25}$$

This is just the same pairing potential in the RPA as derived by KMK.[4,5] [Even if we include phonons into the system, we obtain the result of KMK for $V_p^*(\mathbf{k},\mathbf{k}')$ in the ring approximation. The present author discussed the superconductivity in $SrTiO_3$ in this formalism.[29]] Thus we have found that the KMK pairing potential can be derived, not only from the Eliashberg equation,[7] but also from the present variational procedure.

In the usual KMK scheme, $\tilde{\varepsilon}_{\mathbf{k}}$ and $V_p(\mathbf{k},\mathbf{k}')$ are, respectively, taken to be $\varepsilon_{\mathbf{k}}-\mu_H$ and V_p^* in Eq. (3.25). In our theory, however, we should use Eqs. (1.2) and (1.3) [or at least Eqs. (3.15) and (3.16)] for $\tilde{\varepsilon}_{\mathbf{k}}$ and $V_p(\mathbf{k},\mathbf{k}')$. The difference is the appearance of the renormalization factor $z_{\mathbf{k}}^{-1}$. The correction of the KMK theory by the introduction of $z_{\mathbf{k}}^{-1}$ seems to be quite natural and is consistent with the discussion of Khan and Allen[30] and Schuh and Sham[31] who examined the validity of the KMK approximation.

E. Meaning of the single-particle energy

According to the Landau's Fermi-liquid theory, the single-particle energy $\varepsilon_{\mathbf{k}}^L$ is given by the functional derivative of the total energy in the normal limit with respect to $n_{\mathbf{k}}$. In the RPA, we can rewrite Eq. (3.10) as

$$\Omega^{(0)}=\sum_{\mathbf{k}}2(\varepsilon_{\mathbf{k}}-\mu)n_{\mathbf{k}}-\sum_{\mathbf{k}}\sum_{\mathbf{k}'\neq\mathbf{k}}V(\mathbf{k}-\mathbf{k}')n_{\mathbf{k}}n_{\mathbf{k}'}+\tfrac{1}{2}\sum_{\mathbf{q}\neq0}\int_{-\infty}^{\infty}\frac{d\omega}{2\pi i}\{\ln[1+V(q)\Pi_0(q,\omega)]-V(q)\Pi_0(q,\omega)\} , \tag{3.10'}$$

where

$$\Pi_0(q,\omega)=-\sum_{\mathbf{k}\sigma}\int\frac{d\omega'}{2\pi i}G_{\mathbf{k}}(\omega')G_{\mathbf{k}+\mathbf{q}}(\omega+\omega') , \tag{3.11'}$$

with

$$G_{\mathbf{k}}(\omega')=\frac{n_{\mathbf{k}}}{\omega'-i0^+-\varepsilon_{\mathbf{k}}+\mu_H}+\frac{1-n_{\mathbf{k}}}{\omega'+i0^+-\varepsilon_{\mathbf{k}}+\mu_H} . \tag{3.26}$$

Thus, by taking the same procedure as Rice,[27] we obtain

$$\begin{aligned}\varepsilon_{\mathbf{k}}^L=\frac{1}{2}\frac{\delta\Omega^{(0)}}{\delta n_{\mathbf{k}}}=\varepsilon_{\mathbf{k}}-\mu-\sum_{\mathbf{k}'\neq\mathbf{k}}V(\mathbf{k}-\mathbf{k}')n_{\mathbf{k}'}-\sum_{\mathbf{q}\neq0}\int_{-\infty}^{\infty}\frac{d\omega}{2\pi i}V(q)\left[\frac{1}{1+V(q)\Pi_0(q,\omega)}-1\right]\\\times\left[\frac{n_{\mathbf{k}+\mathbf{q}}}{\omega-i0^+-\varepsilon_{\mathbf{k}}+\varepsilon_{\mathbf{k}+\mathbf{q}}}+\frac{1-n_{\mathbf{k}+\mathbf{q}}}{\omega+i0^+-\varepsilon_{\mathbf{k}}+\varepsilon_{\mathbf{k}+\mathbf{q}}}\right] .\end{aligned} \tag{3.27}$$

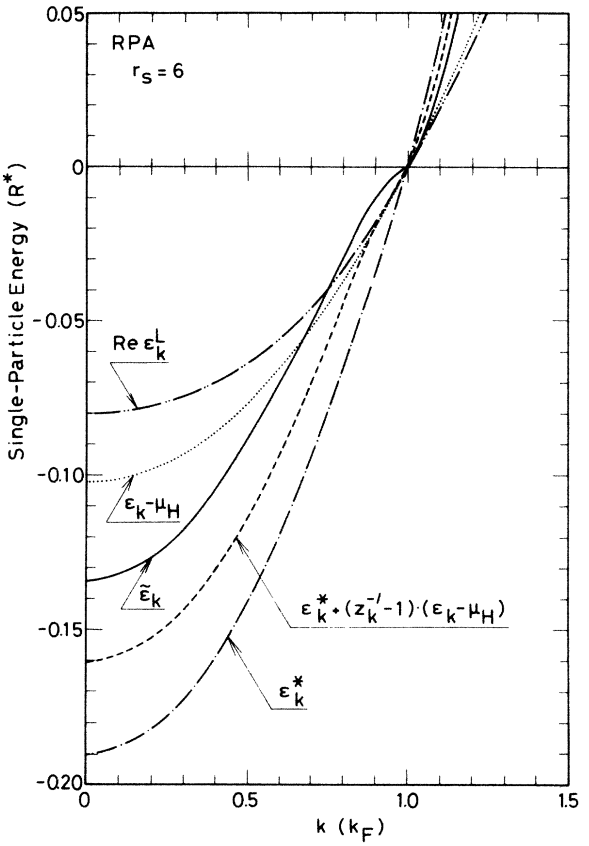

FIG. 2. Various single-particle energies evaluated at $r_s = 6$ in the RPA. Solid, dashed, dotted-dashed, double-dotted-dashed, and dotted curves correspond to, respectively, $\tilde{\varepsilon}_k$ defined in Eq. (1.2), $\tilde{\varepsilon}_k$ in Eq. (3.15), ε_k^* in Eq. (3.17), the real part of ε_k^L in Eq. (3.27), and the bare single-particle energy, $\varepsilon_k - \mu_H$. All energies are in units of R^*.

(Note that the factor $\frac{1}{2}$ in front of $\delta\Omega^{(0)}/\delta n_k$ takes account of the spin factor.) When we compare ε_k^L with ε_k^* in Eq. (3.17) with $\tilde{V}_l(q) = V(q)$, we have

$$\varepsilon_{k_F}^L = \varepsilon_{k_F}^* . \tag{3.28}$$

This indicates that the chemical potential μ can be determined by the calculation of either $\varepsilon_{k_F}^L$ or $\varepsilon_{k_F}^*$; however, they are different for $|\mathbf{k}| \neq k_F$. An example of the calculated results for $\tilde{\varepsilon}_k$ defined in Eq. (1.2), that in Eq. (3.15), ε_k^*, and the real part of ε_k^L is shown in Fig. 2. It is clearly seen that, except at the Fermi surface, neither $\tilde{\varepsilon}_k$ nor ε_k^* is directly connected with the physical single-particle energy ε_k^L.

From a viewpoint of numerical evaluation, ε_k^L has a pole in the integrand, which makes the calculation much more difficult than that for ε_k^*. The same is true for $V_p^*(\mathbf{k},\mathbf{k}')$. For given $\mathbf{k}$ and $\mathbf{k}'$, V_p^* has no singular points in the integrand and is very convenient for numerical calculations. However, V_p^* has no direct physical meaning except at the Fermi surface, i.e., $|\mathbf{k}| = |\mathbf{k}'| = k_F$, at which V_p^* is nothing but a statically screened potential between electrons. Thus we can conclude that in the present variational theory, we have introduced artificial quantities like $\tilde{\varepsilon}_k$ and $V_p(\mathbf{k},\mathbf{k}')$ rather than the real single-particle energy and physical effective potential between the Cooper pair in order to make the numerical evaluation of T_c (or the gap at the Fermi surface at $T=0$) much easier. This situation seems to be quite analogous to that in the density-functional theory[32] in which we use unphysical Kohn-Sham single-particle energy eigenvalues to obtain the physically meaningful charge densities and the ground-state energy.[33] [Although the Kohn-Sham eigenvalues do not represent the real energy levels quantitatively, they quite often give a qualitative structure of the density of states near the Fermi level. Thus we may expect that by evaluating the single-particle energy $(\tilde{\varepsilon}_k^2 + \Delta_k^2)^{1/2}$ at $T=0$, we can obtain at least a qualitative structure of the density of states near the Fermi surface in the superconducting state.]

F. Numerical procedure to obtain T_c

Once $\tilde{\varepsilon}_k$ and $V_p(\mathbf{k},\mathbf{k}')$ are obtained at $T=0$, we can evaluate T_c by solving Eq. (1.6) by the following procedure: Since both Δ_k and $\tilde{\varepsilon}_k$ are a function of $k = |\mathbf{k}|$, we first integrate over the angular parts $\Omega_{k'}$ of the $\mathbf{k}'$ integral in Eq. (1.6). Then we divide the infinite integral for k' into small intervals, (k_i, k_{i+1}). Assuming that Δ_k is constant in each small interval, we can rewrite Eq. (1.6) into

$$\Delta_{\bar{k}_i} = -\sum_j \int_{k_j}^{k_{j+1}} dk' k'^2 \frac{\Delta_{\bar{k}_j}}{2\tilde{\varepsilon}_{k'}} K(\bar{k}_i,\bar{k}_j) \tanh\left[\frac{\tilde{\varepsilon}_{k'}}{2T_c}\right] , \tag{3.29}$$

where $\bar{k}_i \equiv (k_i + k_{i+1})/2$, and the kernel $K(\bar{k}_i,\bar{k}_j)$ is defined by

$$K(\bar{k}_i,\bar{k}_j) = \frac{1}{k_{j+1}-k_j} \times \int_{k_j}^{k_{j+1}} dk' \int \frac{d\Omega_{\mathbf{k}'}}{(2\pi)^3} V_p(\mathbf{k},\mathbf{k}')|_{|\mathbf{k}|=\mathbf{k}_i} . \tag{3.30}$$

Now, for a given T_c, we can define a vector $\mathbf{D}$ and a matrix $\underline{J}$ by

$$\mathbf{D} = (\Delta_{\bar{k}_i}) \tag{3.31}$$

and

$$\underline{J} = \left[-K(\bar{x}_i,\bar{x}_j) \int_{k_j}^{k_{j+1}} dk' \frac{k'^2}{2\tilde{\varepsilon}_{k'}} \tanh\left[\frac{\tilde{\varepsilon}_{k'}}{2T_c}\right] \right] , \tag{3.32}$$

respectively, and consider the following eigenvalue problem:

$$\lambda \mathbf{D} = \underline{J}\mathbf{D} . \tag{3.33}$$

For large enough T_c, all eigenvalues of $\underline{J}$ go to zero. As the trial T_c is decreased, the largest eigenvalue of $\underline{J}$,

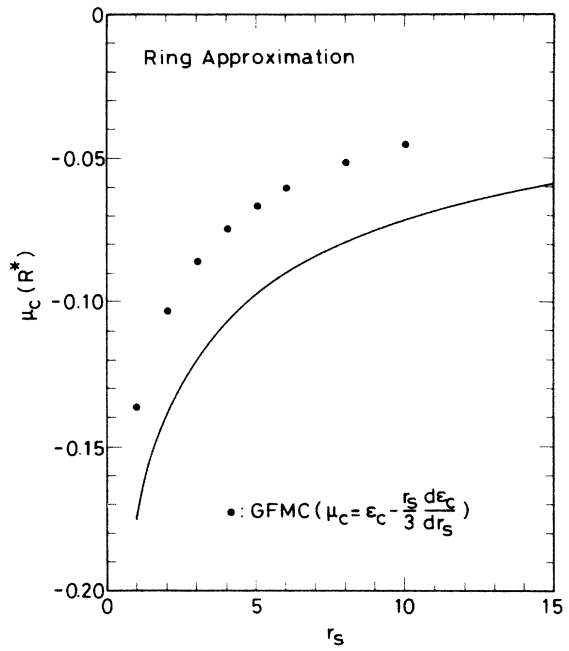

FIG. 3. The correlation part of the chemical potential μ_c in R^* as a function of r_s in the RPA. The solid points indicate the results in the GFMC.

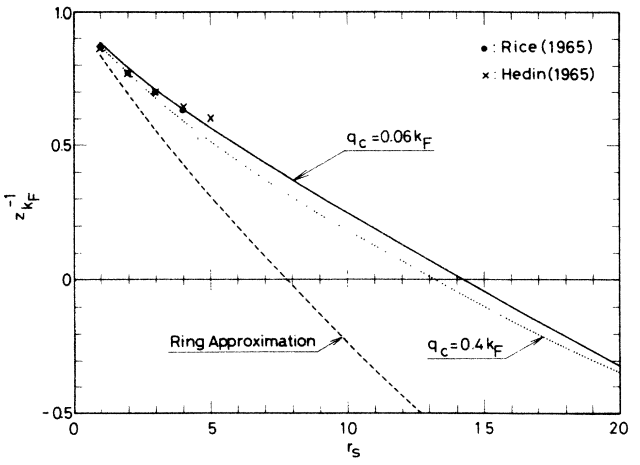

FIG. 4. The renormalization factor at the Fermi surface $z_{k_F}^{-1}$ as a function of r_s. The solid and dotted curves represent the results in the modified two-body approximation with $q_c = 0.06k_F$ and $0.4k_F$, respectively, while the dashed curve shows the results in the RPA. The results given by Rice (Ref. 27) and Hedin (Ref. 28) are also indicated by the solid circles and the crosses, respectively.

λ_{max}, increases. If we can find T_c to make λ_{max} equal to unity, we find a solution of Eq. (3.29) and the assumed T_c is the superconducting transition temperature. (Of course, there are cases in which λ_{max} is always less then unity for any positive T_c. This corresponds to the system in which there is no instability for superconductivity.)

In actual calculations, we have divided the k' integral into one hundred intervals. The smallest interval is taken to be $4\times10^{-7}k_F$ at the Fermi surface. The infinite integral is cut off at $k'=11.2k_F$. We have checked that the relative change of T_c is less than 10^{-2} for other choice of the intervals.

G. Numerical results

For the electron gas, we usually measure wave vectors and energies in units of k_F and $R^*(\equiv m^*e^4/2\epsilon_0^2)$, respectively. Then the system is described by a single parameter r_s, defined by

$$r_s = m^* e^2/\alpha\epsilon_0 k_F \ , \tag{3.34}$$

with $\alpha \equiv (4/9\pi)^{1/3} = 0.521$. In Fig. 3, we give the results for μ_c, defined by

$$\mu_c = \mu - \frac{1}{\alpha^2 r_s^2} + \frac{2}{\pi\alpha r_s} \ , \tag{3.35}$$

as a function of r_s. Compared to the results in the GFMC, μ_c^{GFMC}, the relative error is about 30% at $r_s=1$ and increases up to 58% at $r_s=10$. The results for $z_{k_F}^{-1}$ are given in Fig. 4 by the dashed curve. At $r_s=7.8$, $z_{k_F}^{-1}$ becomes zero, which indicates an occurrence of some metal-insulator-type transition in this approximation.

We have evaluated T_c in various choices of $\tilde{\varepsilon}_{\mathbf{k}}$ and $V_p(\mathbf{k},\mathbf{k}')$. The KMK choice, i.e., $\tilde{\varepsilon}_{\mathbf{k}} = \varepsilon_{\mathbf{k}} - \mu_H$ and $V_p = V_p^*$ in Eq. (3.18), is just the same approximation as in Ref. 4 and reproduces the results in it. In Table I, we have given the results of T_c. In any choice of $\tilde{\varepsilon}_{\mathbf{k}}$ and $V_p(\mathbf{k},\mathbf{k}')$, superconductivity appears with T_c of the order of $0.1K^*$ or higher, when r_s becomes sufficiently large. Here K^* is defined by

TABLE I. Results of T_c in the RPA for various choices of $\tilde{\varepsilon}_k$ and $V_p(\mathbf{k},\mathbf{k}')$. We have not obtained superconductivity for $T_c > 10^{-3}K^*$ when r_s is less than 10 in any choice, where $1K^* = 6.33\times10^{-6}R^*$ with $R^* = m^*e^4/2\epsilon_0^2$. T_c is given in units of K^*. The entries with a dash indicate that we have not obtained superconductivity for $T > 10^{-3}K^*$.

r_s	$\tilde{\varepsilon}_k$ in Eq. (1.2) V_p in Eq. (1.3)	$\tilde{\varepsilon}_k = \varepsilon_k - \mu_H$ V_p in Eq. (1.3)	$\tilde{\varepsilon}_k$ in Eq. (3.15) $V_p = V_p^*$	$\tilde{\varepsilon}_k = \varepsilon_k - \mu_H$ $V_p = V_p^*$ (KMK)
10	–	–	0.037	0.0013
15	–	–	0.080	0.22
20	–	1.4	0.061	0.89
30	0.17	15	0.048	2.1

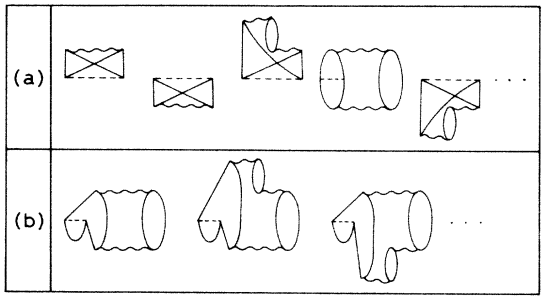

FIG. 5. Goldstone diagrams for (a) the ring-exchange and (b) the self-energy terms in $\Omega^{(0)}$.

$$K^*=6.33\times10^{-6}R^* . \tag{3.36}$$

(In the case in which m^* is m_e and $\epsilon_0=1$, K^* is nothing but 1 K.) Although we have not shown it in Table I, T_c has also been evaluated with $\tilde{\varepsilon}_{\mathbf{k}}$ and $V_p(\mathbf{k},\mathbf{k}')$ in Eqs. (3.15) and (3.16), respectively. The results of T_c are $1.1\times10^4\,K^*$ and $1.4\times10^4 K^*$ for $r_s=6$ and 10. This unreasonably high T_c stems from the unphysical treatment in Eq. (3.16) in which the repulsive part $V(q)$ is reduced by the renormalization effect, while the same reduction factor is not operated on the attractive part, i.e., the second term in Eq. (3.18) for V_p^*.

H. Discussion

In this section, we have performed a first-principles calculation of T_c for the electron gas in the ring approximation. This approximation is found to be very convenient to see that our present theory of superconductivity is an extension of the KMK theory to the strong-coupling region by the inclusion of the renormalization factor in the gap equation. We have obtained the result that superconductivity appears for $r_s>20$ with the exchange of the polarization waves of the electron gas itself between a Cooper pair. However, the effect beyond the ring approximation, usually called the local-field correction, is quite important in such low-density systems. We will treat the effect systematically in Sec. V.

IV. MODIFIED TWO-BODY APPROXIMATION

A. Choice of the long-range part of effective potential

In this section we will perform the calculations outlined in Sec. II C. In the small-q limit, only ring diagrams in Fig. 1 become important. Thus the discussion in Sec. III B indicates that $\tilde{V}_l(q)$ should be equal to $V(q)$. For larger q, it is better to make $\tilde{V}_l(q)$ vanish so that other terms like the ring-exchange [Fig. 5(a)] and the self-energy [Fig. 5(b)] diagrams give negligible contributions compared to the ring diagrams. For the purpose, we assume that $\tilde{V}_l(q)$ has the form

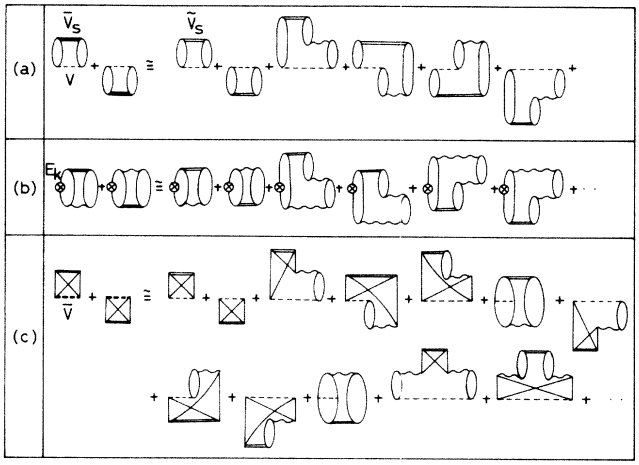

FIG. 6. Goldstone diagrams for $\Omega^{(1)}$.

$$\tilde{V}_l(q)=V(q)\exp(-q^2/q_c^2) , \tag{4.1}$$

in which the cutoff q_c will be determined variationally. We have evaluated the contributions of the terms in Figs. 5(a) and 5(b) with $\tilde{V}_l(q)$ in Eq. (4.1). The ratio of the contribution to that of the ring terms does not exceed 1.0% for q_c smaller than $0.1k_F$. Therefore, as long as we confine ourselves to exploring the optimum q_c in the region less than $0.1k_F$, we can employ the expression for $\Omega^{(0)}$ given in Sec. III A with $\tilde{V}_l(q)$ in the form of Eq. (4.1).

B. First-order term $\Omega^{(1)}$

In Fig. 6, we have given important diagrams for $\Omega^{(1)}$. For the direct processes Figs. 6(a) and 6(b), we can easily obtain the sum of these diagrams by

$$\Omega^{(1d)}=\sum_{\mathbf{q}\neq0}\frac{\delta\Omega^{(0)}}{\delta\tilde{V}_l(q)}\tilde{V}_s(q)=-\tfrac{1}{2}\sum_{\mathbf{q}\neq0}\int\frac{d\omega}{2\pi i}V(q)\tilde{V}_s(q)\Pi(q,\omega)^2/[1+\tilde{V}_l(q)\Pi(q,\omega)]^2$$
$$-\sum_{\mathbf{q}\neq0}\int\frac{d\omega}{2\pi i}\frac{\tilde{V}_s(q)}{[1+\tilde{V}_l(q)\Pi(q,\omega)]^2}\sum_{\mathbf{k}}[(\varepsilon_{\mathbf{k}}-\mu_H)(u_{\mathbf{k}}^2-v_{\mathbf{k}}^2)-2\sum_{\mathbf{q}'\neq0}V(q')u_{\mathbf{k}+\mathbf{q}'}v_{\mathbf{k}+\mathbf{q}'}u_{\mathbf{k}}v_{\mathbf{k}}]$$
$$\times\tilde{\Gamma}^2_{\mathbf{k}+\mathbf{q},\mathbf{k}}\left[\frac{1}{(\omega-i0^+ +e_{\mathbf{k}}+e_{\mathbf{k}+\mathbf{q}})^2}+\frac{1}{(\omega+i0^+ -e_{\mathbf{k}}-e_{\mathbf{k}+\mathbf{q}})^2}\right] . \tag{4.2}$$

In the normal limit, we can use Eq. (3.10) for $\Omega^{(0)}$ and obtain $\Omega^{(1d)}$ as

$$\Omega^{(1d)}=\tfrac{1}{2}\sum_{\mathbf{q}\neq 0}\int_0^\infty \frac{d\omega}{\pi}\Pi_0(q,i\omega)^2[-V(q)+\tilde{V}_l(q)]\tilde{V}_s(q)/[1+\tilde{V}_l(q)\Pi_0(q,i\omega)]^2 \ . \tag{4.3}$$

In the actual evaluation of Eq. (4.3), we introduce a static approximation for the screening function $\varepsilon(q,i\omega)$, defined by

$$\varepsilon(q,i\omega)=1+\tilde{V}_l(q)\Pi_0(q,i\omega) \ , \tag{4.4}$$

and write $\Omega^{(1d)}$ as

$$\Omega^{(1d)}=-\sum_{q\neq 0}\sum_{\mathbf{k}\sigma}\sum_{\mathbf{k}'\sigma'}[V(q)-\tilde{V}_l(q)]\bar{V}_s(q)n_{\mathbf{k}}(1-n_{\mathbf{k}+\mathbf{q}})n_{\mathbf{k}'}(1-n_{\mathbf{k}'+\mathbf{q}})/\Delta(\mathbf{q};\mathbf{k},\mathbf{k}') \ , \tag{4.5}$$

with

$$\bar{V}_s(q)\equiv\tilde{V}_s(q)/\varepsilon(q,0)^2 \tag{4.6}$$

and

$$\Delta(\mathbf{q};\mathbf{k},\mathbf{k}')\equiv e_{\mathbf{k}}+e_{\mathbf{k}+\mathbf{q}}+e_{\mathbf{k}'}+e_{\mathbf{k}'+\mathbf{q}} \ . \tag{4.7}$$

The expression (4.5) is the same as Eq. (13a) for $2C^{(d)}_{1,0}(V)$ in Ref. 18, when $V-\tilde{V}_l$ and $\bar{V}_s$ are replaced by V and $\tilde{V}$, respectively.

In the same spirit of the static approximation, we can give an expression for the exchange process [Fig. 6(c)] as

$$\Omega^{(1e)}=\sum_{\mathbf{q}\neq 0}\sum_{\mathbf{k}\mathbf{k}'}\bar{V}(q)\bar{V}_s(|\mathbf{k}'+\mathbf{k}+\mathbf{q}|)\tilde{\Gamma}_{\mathbf{k}+\mathbf{q},\mathbf{k}}\tilde{\Gamma}_{\mathbf{k}'+\mathbf{q},\mathbf{k}'}\tilde{\Gamma}_{\mathbf{k}+\mathbf{q},\mathbf{k}'}\tilde{\Gamma}_{\mathbf{k}'+\mathbf{q},\mathbf{k}}/\Delta(\mathbf{q};\mathbf{k},\mathbf{k}') \ , \tag{4.8}$$

with

$$\bar{V}(q)\equiv V(q)/\varepsilon(q,0)^2 \ . \tag{4.9}$$

In the normal limit, Eq. (4.8) is rewritten as

$$\Omega^{(1e)}=\sum_{\mathbf{q}\neq 0}\sum_{\mathbf{k}\mathbf{k}'}\sum_{\sigma}\bar{V}(q)\bar{V}_s(|\mathbf{k}'+\mathbf{k}+\mathbf{q}|)n_{\mathbf{k}}(1-n_{\mathbf{k}+\mathbf{q}})n_{\mathbf{k}'}(1-n_{\mathbf{k}'+\mathbf{q}})/\Delta(\mathbf{q};\mathbf{k},\mathbf{k}') \ . \tag{4.10}$$

C. Second-order term $\Omega^{(2)}$

Diagrams for $\Omega^{(2)}$ are drawn in Fig. 7. They will be calculated in the static approximation. The direct term for $\langle\Omega_2\rangle$ is written by

$$\Omega^{(2a)}=\tfrac{1}{2}\sum_{\mathbf{q}\neq 0}\sum_{\mathbf{k}\mathbf{k}'}\bar{V}_s(q)^2\varepsilon(q,0)\tilde{\Gamma}^2_{\mathbf{k}+\mathbf{q},\mathbf{k}}\tilde{\Gamma}^2_{\mathbf{k}'+\mathbf{q},\mathbf{k}'}(E_{\mathbf{k}}+E_{\mathbf{k}+\mathbf{q}}+E_{\mathbf{k}'}+E_{\mathbf{k}'+\mathbf{q}})/\Delta(\mathbf{q};\mathbf{k},\mathbf{k}')^2 \ . \tag{4.11}$$

In Eq. (4.11), the factor $\varepsilon(q,0)$ appears to avoid double counting of the screening factor. In a similar way, we obtain the exchange term for $\langle\Omega_2\rangle$ as

$$\Omega^{(2b)}=-\tfrac{1}{2}\sum_{\mathbf{q}\neq 0}\sum_{\mathbf{k}\mathbf{k}'}\bar{V}_s(q)\bar{V}_s(|\mathbf{q}+\mathbf{k}+\mathbf{k}'|)\tilde{\Gamma}_{\mathbf{k}+\mathbf{q},\mathbf{k}}\tilde{\Gamma}_{\mathbf{k}'+\mathbf{q},\mathbf{k}'}\tilde{\Gamma}_{\mathbf{k}+\mathbf{q},\mathbf{k}'}\tilde{\Gamma}_{\mathbf{k}'+\mathbf{q},\mathbf{k}}(E_{\mathbf{k}}+E_{\mathbf{k}+\mathbf{q}}+E_{\mathbf{k}'}+E_{\mathbf{k}'+\mathbf{q}})/\Delta(\mathbf{q};\mathbf{k},\mathbf{k}')^2 \ , \tag{4.12}$$

the ring term as

$$\Omega^{(2c)}=\sum_{\mathbf{q}\neq 0}\sum_{\mathbf{k}_1\mathbf{k}_2\mathbf{k}_3}V(q)\bar{V}_s(q)^2\varepsilon(q,0)\tilde{\Gamma}^2_{\mathbf{k}_1+\mathbf{q},\mathbf{k}_1}\tilde{\Gamma}^2_{\mathbf{k}_2+\mathbf{q},\mathbf{k}_2}\tilde{\Gamma}^2_{\mathbf{k}_3+\mathbf{q},\mathbf{k}_3}/\Delta(\mathbf{q};\mathbf{k}_1,\mathbf{k}_2)\Delta(\mathbf{q};\mathbf{k}_1,\mathbf{k}_3) \ , \tag{4.13}$$

the first ring-exchange term as

$$\Omega^{(2d)}=\sum_{\mathbf{q}\neq 0}\sum_{\mathbf{k}_1\mathbf{k}_2\mathbf{k}_3}\bar{V}(|\mathbf{k}_2-\mathbf{k}_3|)\bar{V}_s(q)^2\varepsilon(q,0)\tilde{\Gamma}^2_{\mathbf{k}_1+\mathbf{q},\mathbf{k}_1}\tilde{\Gamma}_{\mathbf{k}_2+\mathbf{q},\mathbf{k}_2}\tilde{\Gamma}_{\mathbf{k}_3+\mathbf{q},\mathbf{k}_3}\Gamma_{\mathbf{k}_2+\mathbf{q},\mathbf{k}_3+\mathbf{q}}\Gamma_{\mathbf{k}_2,\mathbf{k}_3}/\Delta(\mathbf{q};\mathbf{k}_1,\mathbf{k}_2)\Delta(\mathbf{q};\mathbf{k}_1,\mathbf{k}_3) \ , \tag{4.14}$$

the second ring-exchange term as

$$\Omega^{(2e)}=-2\sum_{\mathbf{q}\neq 0}\sum_{\mathbf{k}_1\mathbf{k}_2\mathbf{k}_3}\bar{V}(q)\bar{V}_s(q)\bar{V}_s(|\mathbf{k}_1+\mathbf{k}_3+\mathbf{q}|)\varepsilon(q,0)\tilde{\Gamma}_{\mathbf{k}_1+\mathbf{q},\mathbf{k}_1}\tilde{\Gamma}^2_{\mathbf{k}_2+\mathbf{q},\mathbf{k}_2}\tilde{\Gamma}_{\mathbf{k}_3+\mathbf{q},\mathbf{k}_3}\tilde{\Gamma}_{\mathbf{k}_1+q,\mathbf{k}_3}\tilde{\Gamma}_{\mathbf{k}_1,\mathbf{k}_3+\mathbf{q}}/\Delta(\mathbf{q};\mathbf{k}_1,\mathbf{k}_2)\Delta(\mathbf{q};\mathbf{k}_1,\mathbf{k}_3) \ , \tag{4.15}$$

the ring-double-exchange term as

$$\Omega^{(2f)}=-2\sum_{\mathbf{q}\neq 0}\sum_{\mathbf{k}_1\mathbf{k}_2\mathbf{k}_3}\bar{V}(|k_2-k_3|)\bar{V}_s(q)\bar{V}_s(|\mathbf{k}_1+\mathbf{k}_3+\mathbf{q}|)\Gamma_{\mathbf{k}_2+\mathbf{q},\mathbf{k}_3+\mathbf{q}}\Gamma_{\mathbf{k}_2,\mathbf{k}_3}$$
$$\times\tilde{\Gamma}_{\mathbf{k}_1,\mathbf{k}_1+\mathbf{q}}\tilde{\Gamma}_{\mathbf{k}_2,\mathbf{k}_2+\mathbf{q}}\tilde{\Gamma}_{\mathbf{k}_1,\mathbf{k}_3+\mathbf{q}}\tilde{\Gamma}_{\mathbf{k}_1+\mathbf{q},\mathbf{k}_3}/\Delta(\mathbf{q};\mathbf{k}_1,\mathbf{k}_2)\Delta(\mathbf{q};\mathbf{k}_1,\mathbf{k}_3)\ , \tag{4.16}$$

the ladder term as

$$\Omega^{(2g)}=2\sum_{\mathbf{q}\mathbf{q}'}\sum_{\mathbf{k}\mathbf{k}'}\bar{V}(|\mathbf{q}-\mathbf{q}'|)\bar{V}_s(q)\bar{V}_s(q')\Gamma_{\mathbf{k}+\mathbf{q},\mathbf{k}+\mathbf{q}'}\Gamma_{\mathbf{k}'+\mathbf{q},\mathbf{k}'+\mathbf{q}'}\tilde{\Gamma}_{\mathbf{k},\mathbf{k}+\mathbf{q}}\tilde{\Gamma}_{\mathbf{k}',\mathbf{k}'+\mathbf{q}}\tilde{\Gamma}_{\mathbf{k},\mathbf{k}+\mathbf{q}'}\tilde{\Gamma}_{\mathbf{k}',\mathbf{k}'+\mathbf{q}'}/\Delta(\mathbf{q};\mathbf{k},\mathbf{k}')\Delta(\mathbf{q}';\mathbf{k},\mathbf{k}')\ , \tag{4.17}$$

the first ladder-exchange term as

$$\Omega^{(2h)}=-\sum_{\mathbf{q}\mathbf{q}'}\sum_{\mathbf{k}\mathbf{k}'}\bar{V}(|\mathbf{k}+\mathbf{k}'+\mathbf{q}+\mathbf{q}'|)\bar{V}_s(q)\bar{V}_s(q')\Gamma_{\mathbf{k}+\mathbf{q},\mathbf{k}'+\mathbf{q}'}\Gamma_{\mathbf{k}+\mathbf{q}',\mathbf{k}'+\mathbf{q}}\tilde{\Gamma}_{\mathbf{k},\mathbf{k}+\mathbf{q}}\tilde{\Gamma}_{\mathbf{k}',\mathbf{k}'+\mathbf{q}}$$
$$\times\tilde{\Gamma}_{\mathbf{k},\mathbf{k}+\mathbf{q}'}\tilde{\Gamma}_{\mathbf{k}',\mathbf{k}'+\mathbf{q}'}/\Delta(\mathbf{q};\mathbf{k},\mathbf{k}')\Delta(\mathbf{q}';\mathbf{k},\mathbf{k}')\ , \tag{4.18}$$

and, finally, the second ladder-exchange term as

$$\Omega^{(2i)}=\sum_{\mathbf{q}\mathbf{q}'}\sum_{\mathbf{k}\mathbf{k}'}\bar{V}(|\mathbf{k}-\mathbf{k}'|)\bar{V}_s(q)\bar{V}_s(q')\tilde{\Gamma}_{\mathbf{k},\mathbf{k}+\mathbf{q}}\tilde{\Gamma}_{\mathbf{k}',\mathbf{k}'+\mathbf{q}}\tilde{\Gamma}_{\mathbf{k},\mathbf{k}+\mathbf{q}'}\tilde{\Gamma}_{\mathbf{k}',\mathbf{k}'+\mathbf{q}'}$$
$$\times\tilde{\Gamma}_{\mathbf{k}+\mathbf{q},\mathbf{k}'+\mathbf{q}}\tilde{\Gamma}_{\mathbf{k}+\mathbf{q}',\mathbf{k}'+\mathbf{q}'}/\Delta(\mathbf{q};\mathbf{k},\mathbf{k}')\Delta(\mathbf{q}';\mathbf{k},\mathbf{k}')\ . \tag{4.19}$$

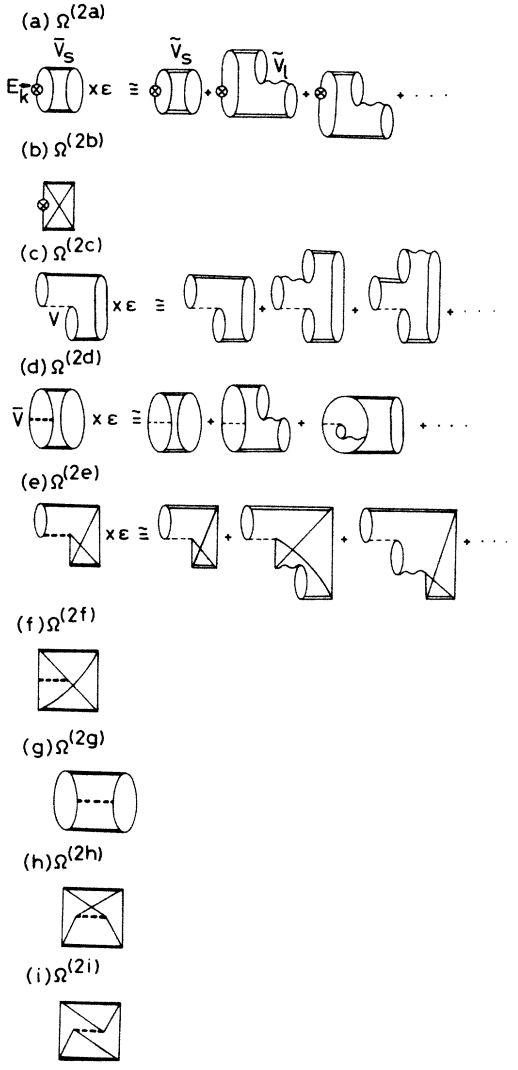

FIG. 7. Goldstone diagrams for $\Omega^{(2)}$. Diagrams associated with the symbol "$\times\varepsilon$" indicate that we should multiply $\varepsilon(q,0)$ in the final expression to avoid double counting of the screening factor.

D. Determination of q_c and $\bar{V}_s$

In the normal limit, all terms in $\Omega^{(1)}$ and $\Omega^{(2)}$ reduce to the expression very similar to that in the two-body approximation.[18,20] Thus we can evaluate $\langle\Omega\rangle$ with the same technique as in the previous works. We take the following procedure to determine q_c and $\bar{V}_s(q)$. First, we give a trial q_c and determine $\bar{V}_s$ by the numerical solution of

$$\frac{\delta\langle\Omega\rangle}{\delta\bar{V}_s(q)}=0\ , \tag{4.20}$$

and calculate $\langle\Omega\rangle$ with $\bar{V}_s(q)$ thus obtained. Next, we change q_c so that we can find a minimum of $\langle\Omega\rangle$ in the region of $0\leq q_c\leq 0.1k_F$.

In Fig. 8, we have plotted the correlation energy of the normal electron gas, ε_c, which is nothing but $(\langle\Omega\rangle-\Omega_0)/N$, where N is the total electron number. For $1\leq r_s\leq 20$, ε_c has a local minimum at $q_c=0.06k_F$. (This value seems to be independent of r_s.) Since this value satisfies the restriction $0\leq q_c\leq 0.1k_F$, we will choose it for q_c in the calculations of physical quantities like z_k, μ_c, and T_c. However, ε_c shows a rather interesting behavior as q_c is increased: Near $q_c\sim 0.15k_F$, ε_c has another local minimum, but for q_c larger than $0.2k_F$, ε_c decreases monotonically and becomes lower than the value in the GFMC for $q_c>0.45k_F$. Thus it is obvious that we should consider terms other than the ring ones in $\tilde{V}_l$ in order to make the variational procedure work even for $q_c>0.2k_F$. However, we may also choose $0.4k_F$ for q_c to calculate physical quantities and compare the calculated results with those for $q_c=0.06k_F$, although we do not have a physically sound reason to choose it for q_c except that ε_c is always very close to the value in the GFMC. An example of the obtained $\bar{V}_s(q)$ is given in Fig. 9 for $r_s=6$. The solid, dotted-dashed, dashed, and dotted curves represent, respectively, the results for $q_c=0.06k_F$, $0.4k_F$, 0 (i.e., in the two-body approximation), and the bare potential.

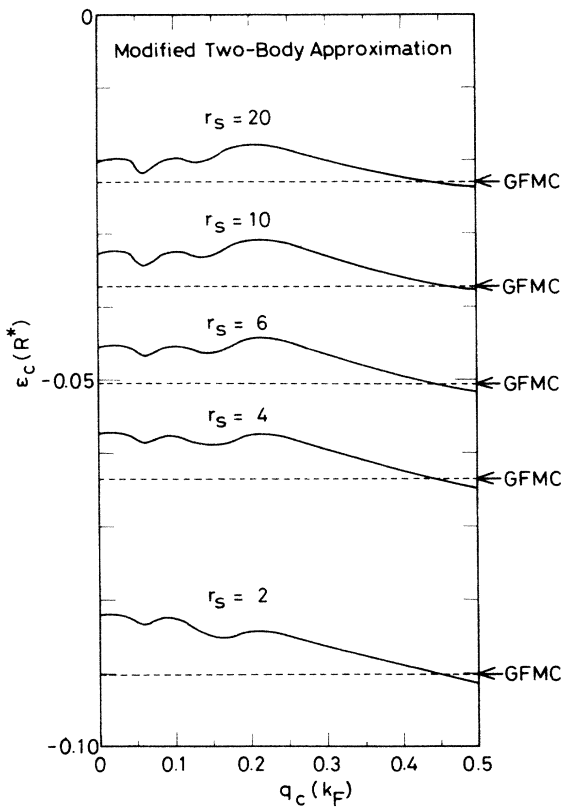

FIG. 8. Correlation energy of the normal electron gas in R^* in the modified two-body approximation as a function of q_c. Cases for $r_s=2$, 4, 6, 10, and 20 are shown. The result in the GFMC for each r_s is indicated by a dashed line.

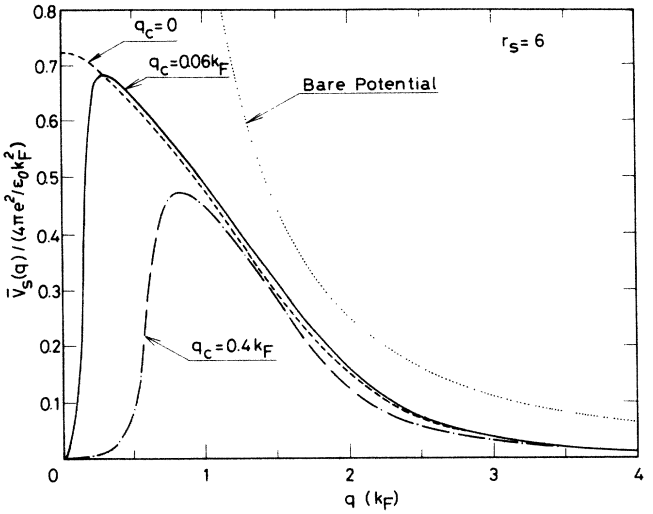

FIG. 9. An example of the calculated short-range part of the effective potential normalized by $4\pi e^2/\epsilon_0 k_F^2$ as a function of q for $r_s=6$. The solid, dotted-dashed, dashed, and dotted curves represent, respectively, the results for $q_c=0.06k_F$, $0.4k_F$, 0 (i.e., in the two-body approximation), and the bare potential.

E. Numerical results for ε_c and the renormalization factor

The obtained minimum values for ε_c with $q_c=0.06k_F$ are given in Table II, together with the values in the two-body approximation and in the GFMC.[19] The relative error between the present results and those in the GFMC is at most 8% for $1\leqq r_s\leqq 20$. Although they are not so good as those in Ref. 20, the present results for ε_c have been much improved on those in the two-body approximation, especially for $r_s>6$.

We can calculate the occupation number $N_{\mathbf{k}}\equiv\langle C^{\dagger}_{\mathbf{k}\sigma}C_{\mathbf{k}\sigma}\rangle$ in the same approximation as that for ε_c. Once we obtain N_k, we can calculate the renormalization factor $z_{\mathbf{k}}^{-1}$ with the use of Eq. (3.23) as

$$z_{\mathbf{k}}^{-1}=1+\Delta z_{\mathbf{k}}+\Delta z_{\mathbf{k}}^{(2d)}+\Delta z_{\mathbf{k}}^{(2e)}\ , \tag{4.21}$$

where $\Delta z_{\mathbf{k}}$ is defined in Eq. (3.19); $\Delta z_{\mathbf{k}}^{(2d)}$ and $\Delta z_{\mathbf{k}}^{(2e)}$ are, respectively, given by

$$\Delta z_{\mathbf{k}}^{(2d)}=-4\sum_{\mathbf{q}\neq 0}\sum_{\mathbf{k}'}\bar{V}_s(q)^2\varepsilon(q,0)\times[n_{\mathbf{k}}(1-n_{\mathbf{k}+\mathbf{q}})+n_{\mathbf{k}+\mathbf{q}}(1-n_{\mathbf{k}})]\times n_{\mathbf{k}'}(1-n_{\mathbf{k}'+\mathbf{q}})/\Delta(\mathbf{q};\mathbf{k},\mathbf{k}')^2 \tag{4.22}$$

and

$$\Delta z_{\mathbf{k}}^{(2e)}=2\sum_{\mathbf{q}\neq 0}\sum_{\mathbf{k}'}\bar{V}_s(q)\bar{V}_s(|\mathbf{q}+\mathbf{k}+\mathbf{k}'|)\times[n_{\mathbf{k}}(1-n_{\mathbf{k}+\mathbf{q}})n_{\mathbf{k}'}(1-n_{\mathbf{k}'+\mathbf{q}})+(1-n_{\mathbf{k}})n_{\mathbf{k}+\mathbf{q}}n_{\mathbf{k}'+\mathbf{q}}(1-n_{\mathbf{k}'})]/\Delta(\mathbf{q};\mathbf{k},\mathbf{k}')^2\ . \tag{4.23}$$

It must be noted that the contribution to $z_{\mathbf{k}}^{-1}$ in first order of $\bar{V}_s(q)$ is given by

TABLE II. Correlation energy ε_c for the normal electron gas in the modified two-body approximation with $q_c=0.06k_F$. The columns indicated by "two-body" and "GFMC" give the results in the two-body approximation and in the GFMC method, respectively. All energies are in R^*.

r_s	ε_c	ε_c (two body)	ε_c (GFMC)
1	−0.113	−0.111	−0.119
2	−0.0834	−0.0821	−0.0902
3	−0.0683	−0.0671	−0.0738
4	−0.0587	−0.0575	−0.0636
5	−0.0520	−0.0506	−0.0563
6	−0.0468	−0.0455	−0.0507
8	−0.0395	−0.0380	−0.0427
10	−0.0344	−0.0329	−0.037 22
15	−0.0265	−0.0249	−0.028 30
20	−0.0219	−0.0203	−0.023 00

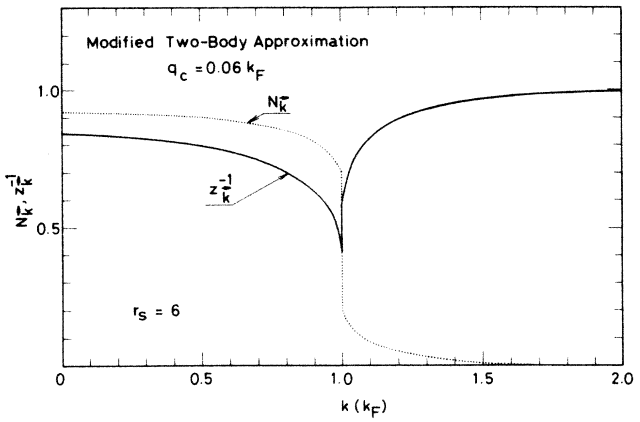

FIG. 10. An example of the occupation number $N_{\mathbf{k}} \equiv \langle C^{\dagger}_{\mathbf{k}\sigma} C_{\mathbf{k}\sigma} \rangle$ (dotted curve) and the renormalization factor $z_{\mathbf{k}}^{-1}$ (solid curve) as a function of $k \equiv |\mathbf{k}|$ for $r_s = 6$.

$$\Delta z_{\mathbf{k}}^{(1)} = \sum_{\mathbf{q}} \int_0^{\infty} \frac{2}{\pi} d\omega \frac{\tilde{V}_s(q)}{[1+\tilde{V}_l(q)\Pi(q,i\omega)]^2} \times [n_{\mathbf{k}}(1-n_{\mathbf{k}+\mathbf{q}}) + n_{\mathbf{k}+\mathbf{q}}(1-n_{\mathbf{k}})] \times \frac{(e_{\mathbf{k}}+e_{\mathbf{k}+\mathbf{q}})^2-\omega^2}{[(e_{\mathbf{k}}+e_{\mathbf{k}+\mathbf{q}})^2+\omega^2]^2} . \tag{4.24}$$

In the static approximation, we may replace $\tilde{V}_s/[1+\tilde{V}_l(q)\Pi_0(q,i\omega)]^2$ by $\bar{V}_s(q)$ and obtain that $\Delta z_{\mathbf{k}}^{(1)}$ vanishes.

In Fig. 10 we have given an example of $N_{\mathbf{k}}$ and $z_{\mathbf{k}}^{-1}$. We have taken $r_s = 6$ and $q_c = 0.06 k_F$. The values of $z_{k_F}^{-1}$ are shown in Fig. 4. The solid and dotted curves correspond to the cases of $q_c = 0.06 k_F$ and $0.4 k_F$, respectively. It is remarkable that although $\bar{V}_s(q)$ for $q_c = 0.4 k_F$ is very different from that for $q_c = 0.06 k_F$ as shown in Fig. 9, the results for $z_{k_F}^{-1}$ do not change so much. When we use $0.06 k_F$ for q_c, the metal-insulator-type transition indicated by $z_{k_F}^{-1} = 0$ does not occur until $r_s = 14.3$. This value is considerably larger than the value $r_s = 7.8$ in the RPA. This difference is due primary to the contribution of the exchange term, $\Delta z_{\mathbf{k}}^{(2e)}$.

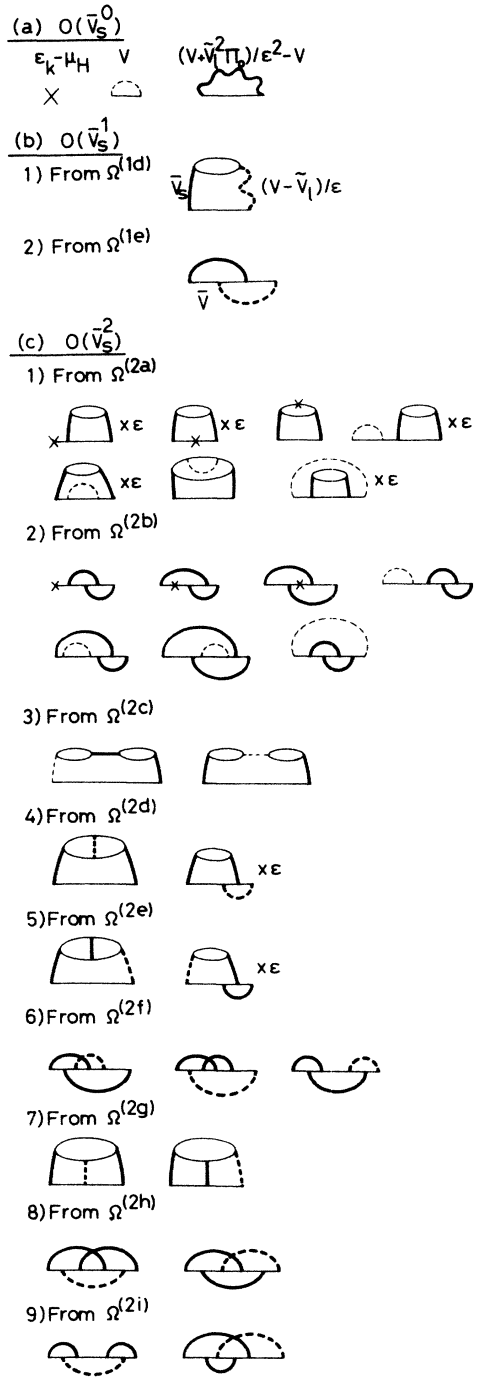

FIG. 11. Diagrammatical representation for $\varepsilon_{\mathbf{k}}^{*}$.

V. SUPERCONDUCTIVITY IN THE ELECTRON GAS

A. Single-particle energy and pairing potential

As in Sec. III C, we can obtain expressions for $\tilde{\varepsilon}_{\mathbf{k}}$ and $V_p(\mathbf{k},\mathbf{k}')$ by taking the functional derivative $\delta\langle\Omega\rangle/\delta v_{\mathbf{k}}$. We will express them in the form of Eqs. (1.2) and (1.3) in which the renormalization factor $z_{\mathbf{k}}^{-1}$ was calculated in Sec. IV E. Contributions to $\varepsilon_{\mathbf{k}}^{*}$ and $V_p^{*}(\mathbf{k},\mathbf{k}')$ from $\Omega^{(0)}$ have already been given in Eqs. (3.17) and (3.18), respectively. [Diagrammatical representations are given in Figs. 11(a) and 12(a).]

The contribution to $\varepsilon_{\mathbf{k}}^{*}$ from $\Omega^{(1d)}$ is given by

$$\varepsilon_{\mathbf{k}}^{(1d)*} = \sum_{\mathbf{q}} \int_0^{\infty} \frac{2}{\pi} d\omega [-V(q)+\tilde{V}_l(q)] \frac{\tilde{V}_s(q)\Pi_0(q,i\omega)}{\varepsilon(q,i\omega)^3} \times \frac{e_{\mathbf{k}}+e_{\mathbf{k}+\mathbf{q}}}{\omega^2+(e_{\mathbf{k}}+e_{\mathbf{k}+\mathbf{q}})^2}(1-2n_{\mathbf{k}+\mathbf{q}}) . \tag{5.1}$$

In the static approximation, Eq. (5.1) is rewritten as

$$\varepsilon_{\mathbf{k}}^{(1d)*} = -4\sum_{\mathbf{q}\mathbf{k}'} \frac{[V(q)-\tilde{V}_l(q)]\bar{V}_s(q)}{\varepsilon(q,0)} \times \frac{(1-2n_{\mathbf{k}+\mathbf{q}})n_{\mathbf{k}'}(1-n_{\mathbf{k}'+\mathbf{q}})}{\Delta(\mathbf{q};\mathbf{k},\mathbf{k}')} . \quad (5.2)$$

Similarly, $\Omega^{(1e)}$ gives $\varepsilon_{\mathbf{k}}^{(1e)*}$ as

$$\varepsilon_{\mathbf{k}}^{(1e)*} = 2\sum_{\mathbf{q}\mathbf{k}'} \bar{V}(q)\bar{V}_s(|\mathbf{q}+\mathbf{k}+\mathbf{k}'|) \times [(1-n_{\mathbf{k}+\mathbf{q}})n_{\mathbf{k}'}(1-n_{\mathbf{k}'+\mathbf{q}}) - n_{\mathbf{k}+\mathbf{q}}(1-n_{\mathbf{k}'})n_{\mathbf{k}'+\mathbf{q}}]/\Delta(\mathbf{q};\mathbf{k},\mathbf{k}') . \quad (5.3)$$

Diagrammatical representations for $\varepsilon_{\mathbf{k}}^{(1d)*}$ and $\varepsilon_{\mathbf{k}}^{(1e)*}$ are shown in Fig. 11(b).

The pairing potential contributed from $\Omega^{(1d)}$ is written as

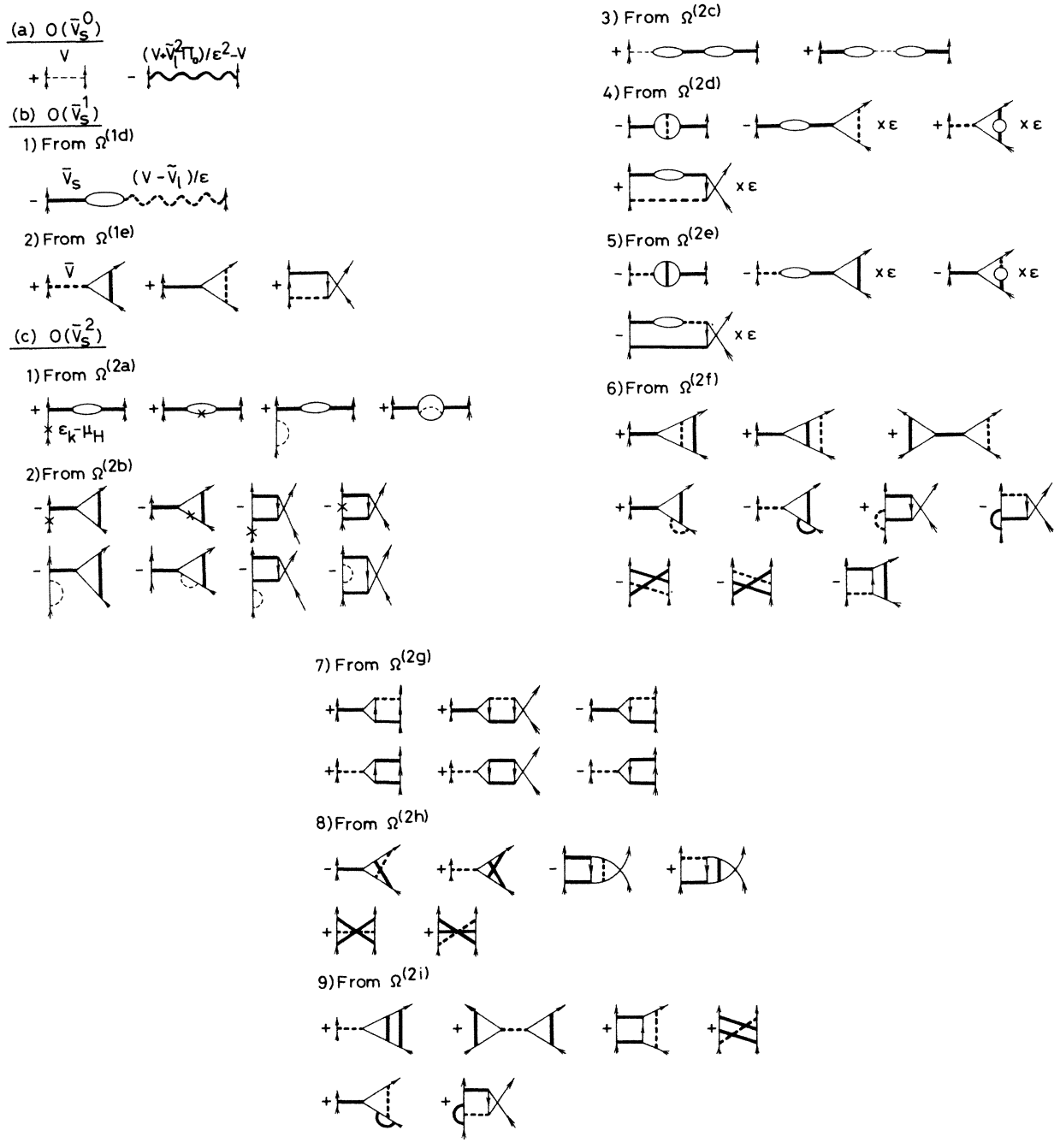

FIG. 12. Diagrammatical representation for $V_p^*(\mathbf{k},\mathbf{k}')$. The plus (+) [minus (−)] sign in front of each diagram indicates repulsive (attractive) contributions to V_p^*.

$$V_p^{(1d)*}(\mathbf{k},\mathbf{k}'\equiv\mathbf{k}+\mathbf{q})=-2\int_0^\infty\frac{2}{\pi}d\omega\frac{e_\mathbf{k}+e_{\mathbf{k}'}}{\omega^2+(e_\mathbf{k}+e_{\mathbf{k}'})^2}[V(q)-\tilde{V}_l(q)]\tilde{V}_s(q)\Pi_0(q,i\omega)/\varepsilon(q,i\omega)^3\ , \tag{5.4}$$

which is rewritten in the static approximation as

$$V_p^{(1d)*}(\mathbf{k},\mathbf{k}'\equiv\mathbf{k}+\mathbf{q})=-8\frac{[V(q)-\tilde{V}_l(q)]\bar{V}_s(q)}{\varepsilon(q,0)}\sum_\mathbf{p}\frac{n_\mathbf{p}(1-n_{\mathbf{p}+\mathbf{q}})}{e_\mathbf{k}+e_{\mathbf{k}'}+e_\mathbf{p}+e_{\mathbf{p}+\mathbf{q}}}\ . \tag{5.5}$$

On the other hand, $\Omega^{(1e)}$ provides the pairing potential as

$$\begin{aligned}V_p^{(1e)*}(\mathbf{k},\mathbf{k}'\equiv\mathbf{k}+\mathbf{q})=&2\bar{V}_s(q)\sum_{\mathbf{q}'}\bar{V}(q')\frac{n_{\mathbf{k}+\mathbf{q}'}(1-n_{\mathbf{k}'+\mathbf{q}'})+n_{\mathbf{k}'+\mathbf{q}'}(1-n_{\mathbf{k}+\mathbf{q}})}{e_\mathbf{k}+e_{\mathbf{k}'}+e_{\mathbf{k}+\mathbf{q}'}+e_{\mathbf{k}'+\mathbf{q}'}}\\&+2\bar{V}(q)\sum_{\mathbf{q}'}\bar{V}_s(q')\frac{n_{\mathbf{k}+\mathbf{q}'}(1-n_{\mathbf{k}'+\mathbf{q}'})+n_{\mathbf{k}'+\mathbf{q}'}(1-n_{\mathbf{k}+\mathbf{q}'})}{e_\mathbf{k}+e_{\mathbf{k}'}+e_{\mathbf{k}+\mathbf{q}'}+e_{\mathbf{k}'+\mathbf{q}'}}\\&+2\sum_{\mathbf{q}'}\bar{V}(q')\bar{V}(|\mathbf{q}'+\mathbf{k}+\mathbf{k}'|)\frac{n_{\mathbf{k}+\mathbf{q}'}(1-n_{\mathbf{k}'+\mathbf{q}'})+n_{\mathbf{k}'+\mathbf{q}'}(1-n_{\mathbf{k}+\mathbf{q}'})}{e_\mathbf{k}+e_{\mathbf{k}'}+e_{\mathbf{k}+\mathbf{q}'}+e_{\mathbf{k}'+\mathbf{q}'}}\ .\end{aligned} \tag{5.6}$$

These contributions to V_p^* are shown diagrammatically in Fig. 12(b).

Although the calculation is tedious, we can calculate the contributions from $\Omega^{(2)}$ in quite a straightforward way. Since it is too lengthy to write down all terms here, we will give only the contributions from the direct term in $\langle\Omega_2\rangle$, i.e., $\Omega^{(2a)}$, the ring term $\Omega^{(2c)}$, and the ladder term $\Omega^{(2g)}$ explicitly. These terms provide relatively compact expressions for $\varepsilon_\mathbf{k}^*$ and V_p^*. All other terms are given only in diagrammatical representations in Figs. 11(c) and 12(c).

From $\Omega^{(2a)}$, we obtain $\tilde{\varepsilon}_\mathbf{k}$ as

$$\begin{aligned}\tilde{\varepsilon}_\mathbf{k}^{(2a)}=&2\sum_{\mathbf{q}\mathbf{k}'}\bar{V}_s(q)^2(1-2n_{\mathbf{k}+\mathbf{q}})\{\varepsilon(q,0)[(1-2n_\mathbf{k})\varepsilon_\mathbf{k}^{(0)}+(1-2n_{\mathbf{k}+\mathbf{q}})\varepsilon_{\mathbf{k}+\mathbf{q}}^{(0)}]+(1-2n_{\mathbf{k}'})\varepsilon_{\mathbf{k}'}^{(0)}+(1-2n_{\mathbf{k}'+\mathbf{q}})\varepsilon_{\mathbf{k}'+\mathbf{q}}^{(0)}\}\\&\times n_{\mathbf{k}'}(1-n_{\mathbf{k}'+\mathbf{q}})/\Delta(\mathbf{q};\mathbf{k},\mathbf{k}')^2+\sum_{\mathbf{k}'}V(\mathbf{k}'-\mathbf{k})\Delta z_{\mathbf{k}'}^{(2d)}(\tfrac{1}{2}-n_{\mathbf{k}'})+\varepsilon_\mathbf{k}^{(0)}\Delta z_\mathbf{k}^{(2d)}\ ,\end{aligned} \tag{5.7}$$

where $\Delta z_\mathbf{k}^{(2d)}$ is defined in Eq. (4.22) and $\varepsilon_\mathbf{k}^{(0)}$ is defined by

$$\varepsilon_\mathbf{k}^{(0)}=\varepsilon_\mathbf{k}-\sum_{\mathbf{k}'}V(\mathbf{k}-\mathbf{k}')n_{\mathbf{k}'}-\mu_H-\mu_X\ , \tag{5.8}$$

with the exchange part of the chemical potential μ_X. The last term in Eq. (5.7) arises from the derivative of $E_\mathbf{k}$ and as explained in Sec. III C, this term should not be included in $\varepsilon_\mathbf{k}^*$. Thus $\varepsilon_\mathbf{k}^{(2a)*}$ is given by the first two terms in Eq. (5.7). Similarly, the pairing potential contributed from $\Omega^{(2a)}$ is written as

$$V_p^{(2d)}(\mathbf{k},\mathbf{k}'\equiv\mathbf{k}+\mathbf{q})=V_p^{(2a)*}(\mathbf{k},\mathbf{k}')+V(q)(\Delta z_\mathbf{k}^{(2d)}+\Delta z_{\mathbf{k}'}^{(2d)})\ , \tag{5.9}$$

where

$$\begin{aligned}V_p^{(2d)*}(\mathbf{k},\mathbf{k}'\equiv\mathbf{k}+\mathbf{q})=&4\sum_\mathbf{p}\bar{V}_s(q)^2\{\varepsilon(q,0)[(1-2n_\mathbf{k})\varepsilon_\mathbf{k}^{(0)}+(1-2n_{\mathbf{k}'})\varepsilon_{\mathbf{k}'}^{(0)}]\\&+(1-2n_\mathbf{p})\varepsilon_\mathbf{p}^{(0)}+(1-2n_{\mathbf{p}+\mathbf{q}})\varepsilon_{\mathbf{p}+\mathbf{q}}^{(0)}\}n_\mathbf{p}(1-n_{\mathbf{p}+\mathbf{q}})/(e_\mathbf{k}+e_{\mathbf{k}'}+e_\mathbf{p}+e_{\mathbf{p}+\mathbf{q}})^2\ .\end{aligned} \tag{5.10}$$

The ring term $\Omega^{(2c)}$ gives the following $\varepsilon_\mathbf{k}^{(2c)*}$ and $V_p^*(\mathbf{k},\mathbf{k}')$:

$$\begin{aligned}\varepsilon_\mathbf{k}^{(2c)*}=&4\sum_\mathbf{q}V(q)\bar{V}_s(q)^2(1-2n_{\mathbf{k}+\mathbf{q}})\left[\sum_\mathbf{p}n_\mathbf{p}(1-n_{\mathbf{p}+\mathbf{q}})/\Delta(\mathbf{q};\mathbf{k},\mathbf{p})\right]^2\\&+8\sum_\mathbf{q}V(q)\bar{V}_s(q)^2(1-2n_{\mathbf{k}+\mathbf{q}})\sum_{\mathbf{p}\mathbf{p}'}n_\mathbf{p}(1-n_{\mathbf{p}+\mathbf{q}})n_{\mathbf{p}'}(1-n_{\mathbf{p}'+\mathbf{q}})/\Delta(\mathbf{q}:\mathbf{k},\mathbf{p})\Delta(\mathbf{q}:\mathbf{p},\mathbf{p}')\end{aligned} \tag{5.11}$$

and

$$V_p^{(2c)*}(\mathbf{k},\mathbf{k}'\equiv\mathbf{k}+\mathbf{q})=8\sum_{\mathbf{p}\mathbf{p}'}V(q)\bar{V}_s(q)^2\frac{n_\mathbf{p}(1-n_{\mathbf{p}+\mathbf{q}})n_{\mathbf{p}'}(1-n_{\mathbf{p}'+\mathbf{q}})}{e_\mathbf{k}+e_{\mathbf{k}'}+e_\mathbf{p}+e_{\mathbf{p}+\mathbf{q}}}\left[\frac{1}{e_\mathbf{k}+e_{\mathbf{k}'}+e_{\mathbf{p}'}+e_{\mathbf{p}'+\mathbf{q}}}+\frac{2}{e_\mathbf{p}+e_{\mathbf{p}+\mathbf{q}}+e_{\mathbf{p}'}+e_{\mathbf{p}'+\mathbf{q}}}\right]\ . \tag{5.12}$$

Finally, the ladder term $\Omega^{(2g)}$ has the following contribution:

$$\varepsilon_{\mathbf{k}}^{(2g)*}=2\sum_{\mathbf{qq'p}}\bar{V}(|\mathbf{q}-\mathbf{q'}|)\bar{V}_s(q)\bar{V}_s(q')[(1-n_{\mathbf{k}+\mathbf{q}})(1-n_{\mathbf{k}+\mathbf{q'}})n_{\mathbf{p}}(1-n_{\mathbf{p}+\mathbf{q}})(1-n_{\mathbf{p}+\mathbf{q'}})+n_{\mathbf{k}+\mathbf{q}}n_{\mathbf{k}+\mathbf{q'}}(1-n_{\mathbf{p}})n_{\mathbf{p}+\mathbf{q}}n_{\mathbf{p}+\mathbf{q'}}$$
$$-n_{\mathbf{k}+\mathbf{q}}n_{\mathbf{k}+\mathbf{q'}}n_{\mathbf{p}}(1-n_{\mathbf{p}+\mathbf{q}})(1-n_{\mathbf{p}+\mathbf{q'}})$$
$$-(1-n_{\mathbf{k}+\mathbf{q}})(1-n_{\mathbf{k}+\mathbf{q'}})(1-n_{\mathbf{p}})n_{\mathbf{p}+\mathbf{q}}n_{\mathbf{p}+\mathbf{q'}}]/\Delta(\mathbf{q};\mathbf{k},\mathbf{p})\Delta(\mathbf{q'};\mathbf{k},\mathbf{p})$$
$$-4\sum_{\mathbf{qq'p}}\bar{V}(q')\bar{V}_s(q)\bar{V}_s(|\mathbf{q}-\mathbf{q'}|)[(1-n_{\mathbf{k}+\mathbf{q}})n_{\mathbf{k}+\mathbf{q'}}(1-n_{\mathbf{p}})n_{\mathbf{p}+\mathbf{q}}(1-n_{\mathbf{p}+\mathbf{q'}})$$
$$+n_{\mathbf{k}+\mathbf{q}}(1-n_{\mathbf{k}+\mathbf{q'}})(1-n_{\mathbf{p}})n_{\mathbf{p}+\mathbf{q}}(1-n_{\mathbf{p}+\mathbf{q'}})-(1-n_{\mathbf{k}+\mathbf{q}})n_{\mathbf{k}+\mathbf{q'}}n_{\mathbf{p}}(1-n_{\mathbf{p}+\mathbf{q}})n_{\mathbf{p}-}$$
$$-n_{\mathbf{k}+\mathbf{q}}(1-n_{\mathbf{k}+\mathbf{q'}})n_{\mathbf{p}}(1-n_{\mathbf{p}+\mathbf{q}})n_{\mathbf{p}+\mathbf{q'}}]/[\Delta(\mathbf{q};\mathbf{k},\mathbf{p})(e_{\mathbf{k}+\mathbf{q}}+e_{\mathbf{k}+\mathbf{q'}}+e_{\mathbf{p}+\mathbf{q}}+e_{\mathbf{p}+\mathbf{q'}})] \tag{5.13}$$

and

$$V_p^{(2g)*}(\mathbf{k},\mathbf{k'}\equiv\mathbf{k}+\mathbf{q})=4\sum_{\mathbf{p},\mathbf{q'}}\frac{\bar{V}(q')\bar{V}_s(q)\bar{V}(|\mathbf{q}+\mathbf{q'}|)}{(e_{\mathbf{k}}+e_{\mathbf{k'}}+e_{\mathbf{p}}+e_{\mathbf{p}+\mathbf{q}})(e_{\mathbf{k}}+e_{\mathbf{k'}+\mathbf{q'}}+e_{\mathbf{p}-\mathbf{q'}}+e_{\mathbf{p}+\mathbf{q}})}$$
$$\times[n_{\mathbf{p}+\mathbf{q}}(1-n_{\mathbf{p}-\mathbf{q'}})(1-n_{\mathbf{p}})(1-n_{\mathbf{k'}+\mathbf{q'}})+(1-n_{\mathbf{p}+\mathbf{q}})n_{\mathbf{p}-\mathbf{q'}}n_{\mathbf{p}}n_{\mathbf{k'}+\mathbf{q'}}$$
$$-(1-n_{\mathbf{p}+\mathbf{q}})n_{\mathbf{p}-\mathbf{q'}}n_{\mathbf{p}}(1-n_{\mathbf{k'}+\mathbf{q'}})-n_{\mathbf{p}+\mathbf{q}}(1-n_{\mathbf{p}-\mathbf{q'}})(1-n_{\mathbf{p}})n_{\mathbf{k'}+\mathbf{q'}}]$$
$$+(\mathbf{k}\leftrightarrow\mathbf{k'}\text{ in the above term})$$
$$+4\sum_{\mathbf{pq'}}\frac{\bar{V}(q)\bar{V}_s(q')\bar{V}_s(|\mathbf{q}-\mathbf{q'}|)}{(e_{\mathbf{k}}+e_{\mathbf{k}+\mathbf{q'}}+e_{\mathbf{p}}+e_{\mathbf{p}+\mathbf{q'}})(e_{\mathbf{k'}}+e_{\mathbf{k}+\mathbf{q'}}+e_{\mathbf{p}+\mathbf{q}}+e_{\mathbf{p}+\mathbf{q'}})}$$
$$\times[(1-n_{\mathbf{p}+\mathbf{q}})(1-n_{\mathbf{p}})(1-n_{\mathbf{k}+\mathbf{q'}})n_{\mathbf{p}+\mathbf{q'}}+n_{\mathbf{p}+\mathbf{q}}n_{\mathbf{p}}n_{\mathbf{k}+\mathbf{q'}}(1-n_{\mathbf{p}+\mathbf{q'}})$$
$$-(1-n_{\mathbf{p}+\mathbf{q}})(1-n_{\mathbf{p}})n_{\mathbf{k}+\mathbf{q'}}n_{\mathbf{p}+\mathbf{q'}}-n_{\mathbf{p}+\mathbf{q}}n_{\mathbf{p}}(1-n_{\mathbf{k}+\mathbf{q'}})(1-n_{\mathbf{p}+\mathbf{q'}})]\ . \tag{5.14}$$

B. Numerical procedure to evaluate $\varepsilon_{\mathbf{k}}^{*}$ and V_p^{*}

We will calculate T_c by the procedure explained in Sec. III F. The key quantity is the kernel $K(\bar{k}_i,\bar{k}_j)$ defined in Eq. (3.30). There are problems in obtaining $K(\bar{k}_i,\bar{k}_j)$ numerically. We have to perform six-dimensional integrals at about ten thousand points. In addition, numerical errors in the evaluation of the integral should be very small. The relative error must be less than 10^{-7} near the Fermi surface, because we need to calculate $K(\bar{k}_i,\bar{k}_j)$ by changing $\bar{k}_i$ by only $4\times10^{-7}k_F$ at $\bar{k}_i\approx k_F$. From such considerations and a numerical test to estimate the computation time, we come to the conclusion that we cannot perform the numerical integrations such as Eq. (5.13) as they are at the present level of computers. Thus we will calculate $\varepsilon_{\mathbf{k}}^{*}$ and V_p^{*} in the following way. (Note that $z_{\mathbf{k}}^{-1}$ is already known.) For the ring terms, $\varepsilon_{\mathbf{k}}^{(1d)*}$, $V_p^{(1d)*}$, $\varepsilon_{\mathbf{k}}^{(2a)*}$, $V_p^{(2a)*}$, $\varepsilon_{\mathbf{k}}^{(2c)*}$, and $V_p^{(2c)*}$, we make rigorous integrations, because these terms can be reduced to at most three-dimensionsl integrals which do not have any singular points in the integrand. For the exchange terms, $\varepsilon_{\mathbf{k}}^{(1e)*}$ and $V_p^{(1e)*}$, we first rewrite Eqs. (5.3) and (5.6) as

$$\varepsilon_{\mathbf{k}}^{(1e)*}=-2\sum_{\mathbf{qk'}}\bar{V}(q)\bar{V}_s(|\mathbf{k}-\mathbf{k'}|)n_{\mathbf{k}+\mathbf{q}}n_{\mathbf{k'}}(1-n_{\mathbf{k'}+\mathbf{q}})/\Delta(\mathbf{q};\mathbf{k},\mathbf{k'})$$
$$+2\sum_{\mathbf{qk'}}\bar{V}(q)\bar{V}_s(|\mathbf{q}+\mathbf{k}+\mathbf{k'}|)(1-n_{\mathbf{k}+\mathbf{q}})n_{\mathbf{k'}}(1-n_{\mathbf{k'}+\mathbf{q}})/\Delta(\mathbf{q};\mathbf{k},\mathbf{k'}) \tag{5.15}$$

and

$$V_p^{(1e)*}(\mathbf{k},\mathbf{k'}\equiv\mathbf{k}+\mathbf{q})=2\sum_{\mathbf{p}}\frac{n_{\mathbf{p}}(1-n_{\mathbf{p}+\mathbf{q}})}{e_{\mathbf{k}}+e_{\mathbf{k'}}+e_{\mathbf{p}}+e_{\mathbf{p}+\mathbf{q}}}\{\bar{V}_s(q)[\bar{V}(|\mathbf{p}+\mathbf{k'}|)+\bar{V}(|\mathbf{p}-\mathbf{k}|)]$$
$$+\bar{V}(q)[\bar{V}_s(|\mathbf{p}+\mathbf{k'}|)+\bar{V}_s(|\mathbf{p}-\mathbf{k}|)]$$
$$+\bar{V}(|\mathbf{p}+\mathbf{k'}|)\bar{V}_s(|\mathbf{p}-\mathbf{k}|)+\bar{V}(|\mathbf{p}-\mathbf{k}|)\bar{V}_s(|\mathbf{p}+\mathbf{k'}|)\}\ , \tag{5.16}$$

respectively. Next, in Eq. (5.15), we replace $\bar{V}_s(|\mathbf{k}-\mathbf{k}'|)$ and $\bar{V}_s(|\mathbf{q}+\mathbf{k}+\mathbf{k}'|)$ by $\bar{V}_s([\mathbf{k}^2+\langle k\rangle^2]^{1/2})$ and $\bar{V}_s([(\mathbf{k}+\mathbf{q})^2+\langle k\rangle^2]^{1/2})$. Here $\langle k\rangle$ is considered to give an average value of $\mathbf{k}'\equiv|\mathbf{k}'|$ in the $\mathbf{k}'$ integral. After the replacement, Eq. (5.15) gives an integral which is essentially the same as the one for $\varepsilon_{\mathbf{k}}^{(1d)*}$ in Eq. (5.2). Similarly, $V_p^{(1e)*}$ is evaluated approximately by the replacement of $|\mathbf{p}-\mathbf{k}|$ and $|\mathbf{p}+\mathbf{k}'|$ by $(\langle k\rangle^2+\mathbf{k}^2)^{1/2}$ and $(\langle k\rangle^2+\mathbf{k}'^2)^{1/2}$, respectively, in Eq. (5.16).

We will employ the same approximation to evaluate other terms in $\varepsilon_{\mathbf{k}}^*$ and V_p^*. Namely, we will use some average value for the interactions in the integrand by introducing $\langle k\rangle$ in their arguments, but the Fermi factors, i.e., $n_{\mathbf{k}'}(1-n_{\mathbf{k}'+\mathbf{q}})$, and the energy denominators will be treated as rigorously as possible. For example, the ladder term $V_p^{(2g)*}$ is calculated by changing Eq. (5.14) into

$$
\begin{aligned}
V_p^{(2g)*}(\mathbf{k},\mathbf{k}')=4\sum_{\mathbf{p}\mathbf{p}'}\frac{n_{\mathbf{p}}(1-n_{\mathbf{p}+\mathbf{q}})}{e_{\mathbf{k}}+e_{\mathbf{k}'}+e_{\mathbf{p}}+e_{\mathbf{p}+\mathbf{q}}}\bar{V}_s(q)
&\times\left[\bar{V}_s\left(\left|\mathbf{p}'-\frac{\mathbf{p}+\mathbf{k}}{2}\right|\right)\bar{V}\left(\left|\mathbf{p}'-\mathbf{k}'-\frac{\mathbf{p}-\mathbf{k}}{2}\right|\right)\right.\\
&\times(1-n_{\mathbf{p}'-(\mathbf{p}-\mathbf{k})/2})(1-n_{\mathbf{p}'+(\mathbf{p}-\mathbf{k})/2})/(e_{\mathbf{k}}+e_{\mathbf{p}}+e_{\mathbf{p}'-(\mathbf{p}-\mathbf{k})/2}+e_{\mathbf{p}'+(\mathbf{p}-\mathbf{k})/2})\\
&+\bar{V}_s\left(\left|\mathbf{p}'-\mathbf{k}+\frac{\mathbf{p}+\mathbf{k}'}{2}\right|\right)\bar{V}\left(\left|\mathbf{p}'+\frac{\mathbf{p}-\mathbf{k}'}{2}\right|\right)\\
&\times n_{\mathbf{p}'-(\mathbf{p}+\mathbf{k}')/2}n_{\mathbf{p}'+(\mathbf{p}+\mathbf{k}')/2}/(e_{\mathbf{k}}+e_{\mathbf{p}+\mathbf{q}}+e_{\mathbf{p}'+(\mathbf{p}+\mathbf{k}')/2}+e_{\mathbf{p}'-(\mathbf{p}+\mathbf{k}')/2})\\
&-\bar{V}_s\left(\left|\mathbf{p}'-\frac{\mathbf{p}+\mathbf{k}}{2}\right|\right)\bar{V}\left(\left|\mathbf{p}-\mathbf{k}'-\frac{\mathbf{p}-\mathbf{k}}{2}\right|\right)\\
&\times n_{\mathbf{p}'-(\mathbf{p}-\mathbf{k})/2}(1-n_{\mathbf{p}'+(\mathbf{p}-\mathbf{k})/2})/(e_{\mathbf{k}}+e_{\mathbf{p}}+e_{\mathbf{p}'-(\mathbf{p}-\mathbf{k})/2}+e_{\mathbf{p}'+(\mathbf{p}-\mathbf{k})/2})\\
&-\bar{V}_s\left(\left|\mathbf{p}'-\mathbf{k}+\frac{\mathbf{p}+\mathbf{k}'}{2}\right|\right)\bar{V}\left(\left|\mathbf{p}'+\frac{\mathbf{p}-\mathbf{k}'}{2}\right|\right)\\
&\left.\times n_{\mathbf{p}'-(\mathbf{p}+\mathbf{k}')/2}(1-n_{\mathbf{p}'+(\mathbf{p}+\mathbf{k}')/2})/(e_{\mathbf{k}}+e_{\mathbf{p}+\mathbf{q}}+e_{\mathbf{p}'+(\mathbf{p}+\mathbf{k}')/2}+e_{\mathbf{p}'-(p+\mathbf{k}')/2})\right],
\end{aligned}
\tag{5.17}
$$

and then by replacing $|\mathbf{p}'-(\mathbf{p}+\mathbf{k})/2|$, $|\mathbf{p}'-\mathbf{k}'-(\mathbf{p}-\mathbf{k})/2|$, etc., with $(p'^2+\langle k\rangle^2/4+\mathbf{k}^2/4)^{1/2}$, $(p'^2+\mathbf{k}'^2+\langle k\rangle^2/4+\mathbf{k}^2/4)^{1/2}$, etc.

As for the choice of $\langle k\rangle$, let us consider the integral

$$
\langle(\mathbf{k}-\mathbf{k}')^2\rangle\equiv\sum_{\mathbf{k}'}(\mathbf{k}-\mathbf{k}')^2n_{\mathbf{k}'}(1-n_{\mathbf{k}'+\mathbf{q}})\Big/\sum_{\mathbf{k}'}n_{\mathbf{k}'}(1-n_{\mathbf{k}'+\mathbf{q}})\,. \tag{5.18}
$$

For q larger than $2k_F$, Eq. (5.18) is evaluated as

$$
\langle(\mathbf{k}-\mathbf{k}')^2\rangle=\mathbf{k}^2+\tfrac{3}{5}k_F^2\,, \tag{5.19}
$$

Thus we should choose $\sqrt{3/5}k_F\approx0.775k_F$ for $\langle k\rangle$. For q smaller than $2k_F$, the integral has a complicated form, depending on $k\equiv|\mathbf{k}|$, $\mathbf{k}\cdot\mathbf{q}$, and q, but it is clear that $\langle k\rangle$ approaches k_F for very small q. Actually, we have performed the integral in Eq. (5.14) as it is for several values of k and compared the results with the approximate ones for various choices of $\langle k\rangle$. The best choice for $\langle k\rangle$ is found to be $0.78k_F$. However, it is probably true for other more complicated terms in $\varepsilon_{\mathbf{k}}^*$ and V_p^* that the optimum value for $\langle k\rangle$ is different from $0.78k_F$. Therefore, we will calculate $\varepsilon_{\mathbf{k}}^*$ and V_p^* for several values of $\langle k\rangle$ and show how the physical quantities like μ_c and T_c depend on $\langle k\rangle$.

C. Numerical results

In Fig. 13, we have shown the calculated results for μ_c as a function of r_s for the cases of $\langle k\rangle=0.70k_F$, $0.78k_F$, and $0.85k_F$. The results in the GFMC are indicated by the solid points. These values are reproduced quite well for $1\leq r_s\leq10$, when we choose $0.75k_F$ for $\langle k\rangle$. For the preferred value $\langle k\rangle=0.78k_F$ (the solid curve in Fig. 13), the difference with the results in the GFMC is less than 7% for $r_s\leq10$. Although μ_c depends rather strongly on $\langle k\rangle$, the single-particle energy $\tilde{\varepsilon}_k$ is virtually independent of it as shown in Figs. 14(a) and 14(b) for the cases of $r_s=5$ and 8. For the latter case, we can see a difference in $\tilde{\varepsilon}_{\mathbf{k}}$ for $k<0.3k_F$ and $k>1.3k_F$ with the change of $\langle k\rangle$, but for $r_s=5$ we cannot notice any difference on a scale of the figure.

An example of the calculated kernel $K(\bar{k}_i,\bar{k}_j)$ is

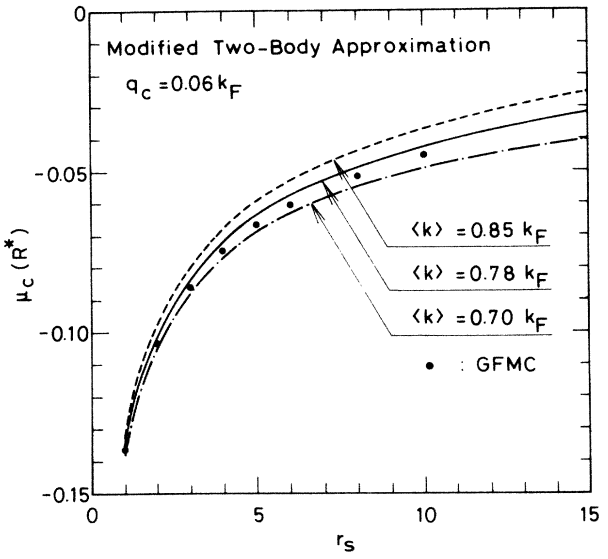

FIG. 13. Calculated results for μ_c in R^* as a function of r_s in the modified two-body approximation with $q_c = 0.06k_F$. The solid points give the results in the GFMC, while the dotted-dashed, solid, and dashed curves correspond to, respectively, the cases for $\langle k \rangle = 0.70k_F$, $0.78k_F$, and $0.85k_F$.

drawn in Fig. 15 in which r_s is taken to be 5, $\bar{k}_i$ is fixed to be $0.999\,999\,8k_F$, and $\bar{k}_j$ is swept. When $\langle k \rangle$ is decreased, the kernel hardly changes its shape, but shifts upwards. In particular, for $\langle k \rangle = 0.78k_F$ (the solid curve in Fig. 15), the calculated kernel at the Fermi surface is about the same as that in the RPA (the dotted curve in Fig. 15). As $\bar{k}_j$ moves away from the Fermi surface, the present kernel is much more repulsive than that in the RPA. Although superconductivity does not appear in the RPA for $r_s = 5$, we have obtained a finite T_c in the present approximation even for $\langle k \rangle = 0.70k_F$. (The values of T_c are given in K^* in Fig. 15.) This example illustrates that superconductivity occurs even if the kernel is always positive for any $\bar{k}_i$ and $\bar{k}_j$. In particular, we cannot discuss the occurrence of superconductivity only by the examination of the pairing potential at the Fermi surface. The important point is that the kernel should change very rapidly near the Fermi surface to have a strong superconducting instability.

The gap function $\Delta_{\mathbf{k}}$ normalized by the value at the Fermi surface Δ_{k_F} is given in Fig. 16. This function has a discontinuous jump at the Fermi surface. This is due to the similar jump in the renormalization factor $z_{\mathbf{k}}^{-1}$. Thus we have defined Δ_{k_F} by

$$\Delta_{k_F} = \tfrac{1}{2}(\Delta_{k_F - 0^+} + \Delta_{k_F + 0^+}) \ . \tag{5.20}$$

The absolute value of Δ_{k_F} cannot be determined by Eq. (1.6). We estimate this from T_c by the BCS relation:[21]

$$\Delta_{k_F} = 1.764 k_B T_c \ . \tag{5.21}$$

In Fig. 17, we have plotted the excitation energy $(\tilde{\varepsilon}_k^2 + \Delta_k^2)^{1/2}$ at $T = 0$ for $r_s = 5$ (the solid curve in Fig.

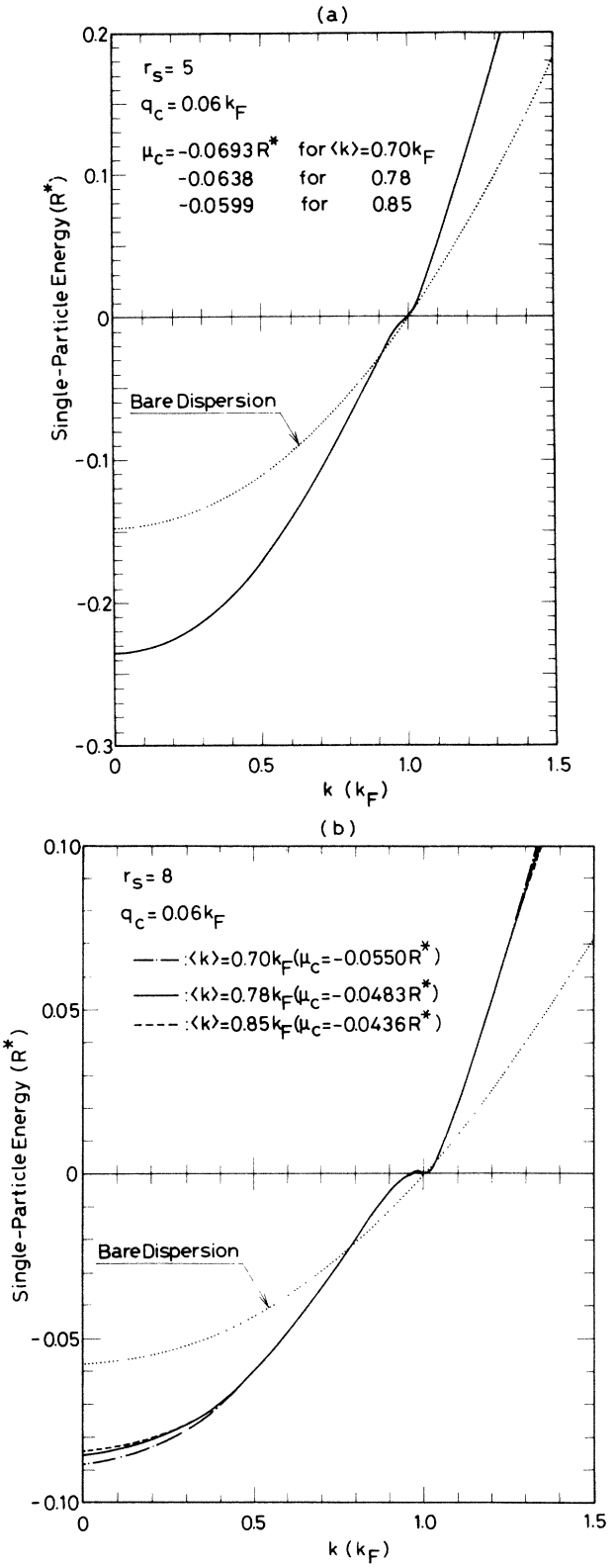

FIG. 14. Single-particle energy in R^* as a function of k for the cases of (a) $r_s = 5$ and (b) $r_s = 8$. Solid curves give the results for $\langle k \rangle = 0.78k_F$. Results for other choices of $\langle k \rangle$ are given by the dashed ($\langle k \rangle = 0.85k_F$) and dotted-dashed ($\langle k \rangle = 0.70k_F$) curves, but in (a) there are no noticeable differences with the change of $\langle k \rangle$. The bare single-particle energy $\varepsilon_{\mathbf{k}} - \mu_H$ is shown by the dotted curve in each case.

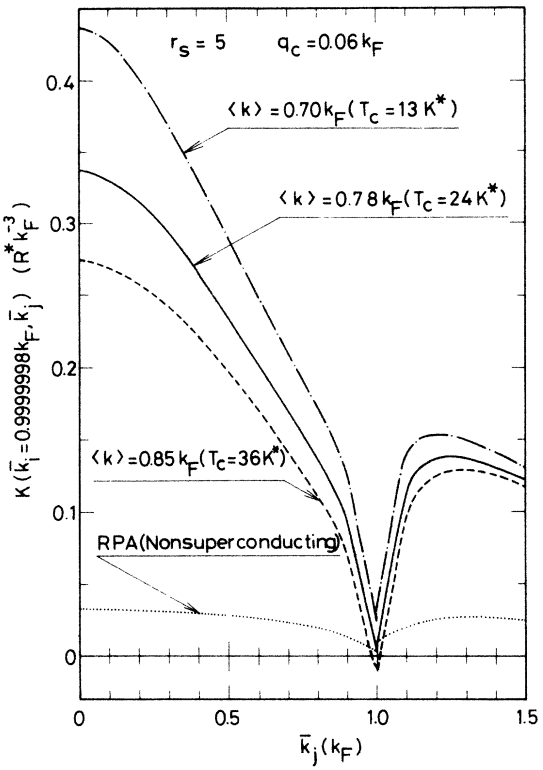

FIG. 15. An example of the calculated kernel $K(\bar{k}_i, \bar{k}_j)$ at $\bar{k}_i = 0.999\,999\,8 k_F$ in units of $R^* k_F^{-3}$. Cases of $\langle k \rangle = 0.70 k_F$, $0.78 k_F$, and $0.85 k_F$ are shown by the dotted-dashed, solid, and dashed curves, respectively. Corresponding results in the RPA are given by the dotted curve.

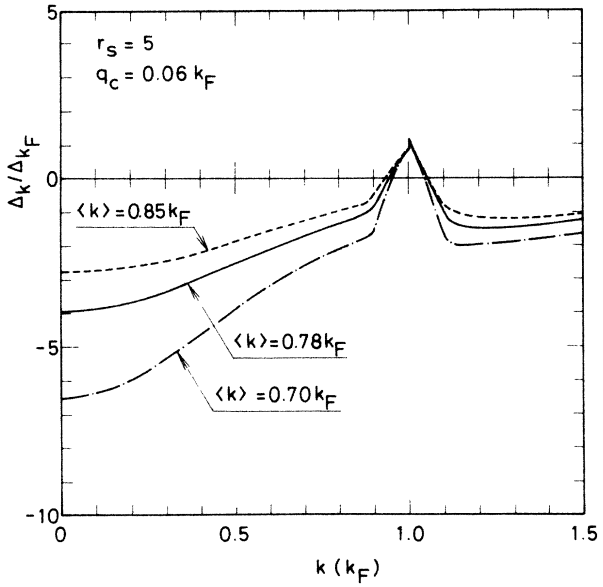

FIG. 16. The gap function Δ_k normalized by Δ_{k_F} for $r_s = 5$. The dotted-dashed, solid, and dashed curves give, respectively, the results for $\langle k \rangle = 0.70 k_F$, $0.78 k_F$, and $0.85 k_F$.

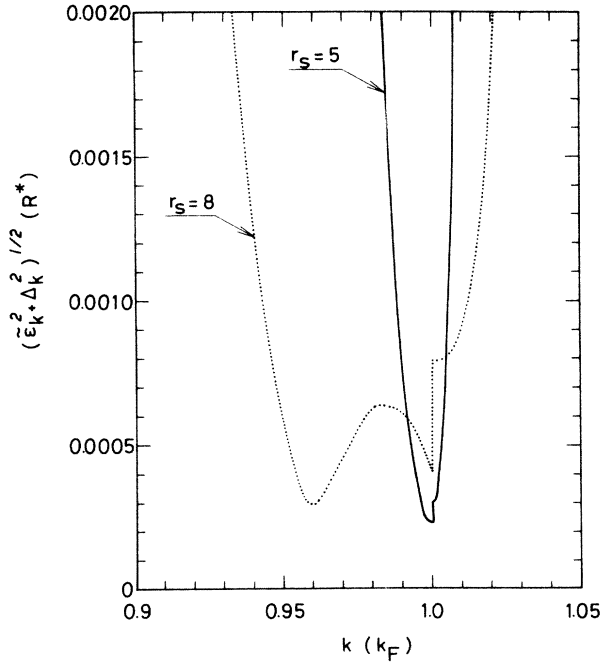

FIG. 17. The excitation energy $(\tilde{\varepsilon}_k^2 + \tilde{\Delta}_k^2)^{1/2}$ in R^* near the Fermi surface at $T = 0$. We have taken $0.78 k_F$ for $\langle k \rangle$ and plotted the cases for $r_s = 5$ and 8 by the solid and dotted curves, respectively.

17) and 8 (the dashed curve in Fig. 17), in which $\langle k \rangle$ is taken to be $0.78 k_F$ and Δ_k is given in Fig. 16 together with Δ_k in Eq. (5.21). Except for the jump at the Fermi surface (which will disappear at finite temperatures), the excitation energy behaves just as a usual BCS superconductor for $r_s = 5$, but two extrema appear in addition to one at the Fermi surface for $r_s = 8$. This is due to the change in sign of $\tilde{\varepsilon}_k$, as seen in Fig. 14(b). If this excitation energy spectrum is true qualitatively, the density of states might show divergence at three different energies near the Fermi surface (it might diverge at four points instead of three, because the excitation energy has a very small slope for $k = k_F + 0^+$).

We have given the results for T_c as a function of r_s in Fig. 18. For the single-particle energy in the gap equation, we have used $\tilde{\varepsilon}_k$ in Fig. 18(a), but for comparison's sake, we have employed the bare one $\varepsilon_k - \mu_H$ in Fig. 18(b). We have chosen $\langle k \rangle$ in three ways as $0.70 k_F$, $0.78 k_F$, and $0.85 k_F$. All these calculations give essentially the same results: Superconductivity appears in the electron gas for $r_s > 3.9$. As r_s increases, T_c increases first, reaches its maximum at $r_s = 7.2$, and then decreases. We have not given T_c for $r_s > 14.3$, because $z_{k_F}^{-1}$ becomes negative in that region of r_s, indicating some metal-insulator-type transition. The peak value of T_c depends on $\langle k \rangle$, but it is in the range $10-100 K^*$. We have also calculated T_c with $q_c = 0.40 k_F$. Qualitative features of the results are the same, but quantitatively, there is a difference: superconductivity appears for $r_s > 6$. The maximum T_c occurs at $r_s = 10$ and is in the range $1-10 K^*$.

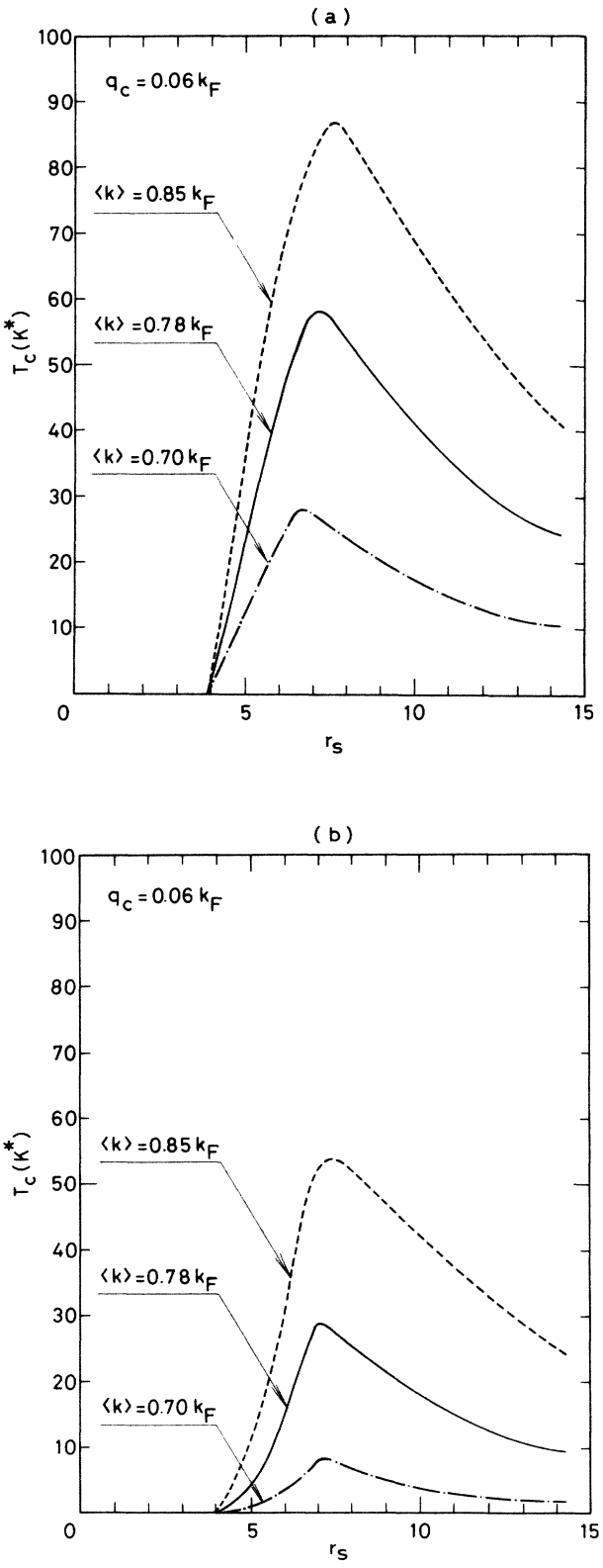

FIG. 18. Calculated results for T_c in units of K^* for the electron gas as a function of r_s in the modified two-body approximation with $q_c = 0.06k_F$. The full single-particle energy $\tilde{\varepsilon}_k$ is used in (a) but the bare one $\varepsilon_k - \mu_H$ is used in (b). Cases of $\langle k \rangle = 0.70k_F$, $0.78k_F$, and $0.85k_F$ are shown by the dotted-dashed, solid, and dashed curves, respectively.

The coherence length ξ_0 at $T=0$ can be estimated by the range of the k-value at which the excitation energy is significantly modified from the normal-state value by the appearance of superconductivity. From Fig. 17, we can see immediately that ξk_F is about 100 and 20 for $r_s = 5$ and 8, respectively. This value $\xi_0 k_F$ decreases rapidly with the further increase of r_s. At $r_s = 14$ this value is about 5.

D. Consideration on mechanism of superconductivity

Compared to the results in the ring approximation in Sec. III, we have seen that, as a whole, the inclusion of the local-field correction brings about a stronger instability for superconductivity in the electron gas. However, there are 56 terms in V_p^* as shown in Fig. 12, and it is not conceivable that all of them are important. Thus we have examined how T_c is affected when we exclude some terms in V_p^* for the calculation of the kernel $K(\bar{k}_i, \bar{k}_j)$ intentionally.

The most important term to overcome the bare repulsive potential $V(q)$ is, of course, $V_p^{(1d)*}$, which includes the plasmon-mediated attractive interaction. However, this term is partially compensated by the contribution of $V_p^{(2a)*}$ and $V_p^{(2c)*}$. Furthermore, the repulsive contribution of $V_p^{(1e)*}$ is so large that superconductivity does not appear without some additional help from other terms. This is true even after we include the contribution of $V_p^{(2b)*}$ to compensate for $V_p^{(1e)*}$. There are three terms in $V_p^{(1e)*}$. The first two terms are the contributions of the vertex correction to the plasmon-mediated interaction (or the exchange effect between the polarization cloud and one electron of a Cooper pair), and the last one represents the paramagnon-mediated interaction. In Fig. 19, we have plotted the change of the kernel from the full calculation which is given by the solid curve. (We have treated the case in which $r_s = 5$, $q_c = 0.06k_F$, and $\langle k \rangle = 0.78k_F$.) The dashed curve corresponds to the kernel without the vertex-correction part of $V_p^{(1e)*}$ and $V_p^{(2b)*}$. We can see that the net effect of the vertex correction is to shift the kernel upwards almost independently of $\bar{k}_j$. This effect is quite harmful to the occurrence of superconductivity. On the other hand, although it has a positive sign, the paramagnon-mediated interaction is, in fact, favorable for superconductivity because this interaction gives a sizable repulsive contribution only when $\bar{k}_i$ and/or $\bar{k}_j$ is not near k_F, as illustrated by the dotted curve in Fig. 19. Since the gap function Δ_k is negative for k not close to k_F, the larger repulsive potential in such a region of k causes the stronger superconducting instability if the kernel near the Fermi surface is about the same. It must be noted here that though we have used the word "paramagnon," the actual contribution comes from the spin fluctuation with the momentum transfer of the order of k_F or larger for the kernel $K(\bar{k}_i, \bar{k}_j)$ in the region where $\bar{k}_i$ and/or $\bar{k}_j$ is not near k_F.

The dotted-dashed curve in Fig. 19 represents the kernel without the first term in $V_p^{(2e)*}$ which is given by

$$V_p^{(2e:1)*}(\mathbf{k},\mathbf{k}'\equiv\mathbf{k}+\mathbf{q})=-8\sum_{\mathbf{pp}'}\bar{V}(q)\bar{V}_s(q)\bar{V}_s(\,|\,\mathbf{p}+\mathbf{p}'+\mathbf{q}\,|\,)\frac{n_{\mathbf{p}}(1-n_{\mathbf{p}+\mathbf{q}})n_{\mathbf{p}'}(1-n_{\mathbf{p}'+\mathbf{q}})}{(e_{\mathbf{k}}+e_{\mathbf{k}'}+e_{\mathbf{p}}+e_{\mathbf{p}+\mathbf{q}})(e_{\mathbf{p}}+e_{\mathbf{p}+\mathbf{q}}+e_{\mathbf{p}'}+e_{\mathbf{p}'+\mathbf{q}})}\ . \tag{5.22}$$

It is found that without this term superconductivity does not appear at $r_s=5$, even if we take into account all of the other 55 terms. In order to see what physical process is involved in $V_p^{(2e:1)*}$, we have to remember the nature of $\bar{V}_s(q)$ determined from the solution of Eq. (4.20).[18] For small q compared to k_F, $\bar{V}_s(q)$ is essentially the same as the screened potential in the Thomas-Fermi type, but for large q, $\bar{V}_s(q)$ takes account of the ladder process. (For q values in between, $\bar{V}_s(q)$ interpolates these two limiting behaviors, together with the inclusion of various exchange terms.) In Eq. (5.22), there are two $\bar{V}_s$'s: For $\bar{V}_s(q)$, the small-q region is important, while for $\bar{V}_s(\,|\,\mathbf{p}+\mathbf{p}'+\mathbf{q}\,|\,)$, the ladder process is dominant. Thus, the important physical process involved in $V_p^{(2e:1)*}$ is the type illustrated diagrammatically in Fig. 20. This represents the exchange of the polarization waves in which the strength of the polarization is enhanced by the electron-hole multiple scatterings.

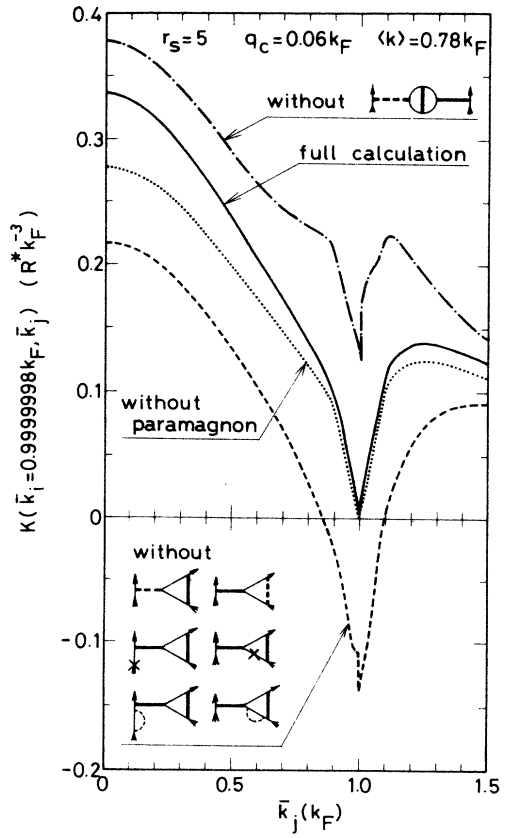

FIG. 19. The kernel $K(\bar{k}_i,\bar{k}_j)$ at $\bar{k}_i=0.999\,999\,8k_F$ in units of $R^*k_F^{-3}$ with the omission of some of terms in $V_p^*(\mathbf{k},\mathbf{k}')$. The solid curve represents the full calculation, while the dashed, dotted, and dotted-dashed curves show the results without the vertex correction, the paramagnon-mediated interaction, and $V_p^{(2e:1)*}$ given in Eq. (5.22), respectively. We have taken $r_s=5$, $q_c=0.06k_F$, and $\langle k\rangle=0.78k_F$.

VI. DISCUSSION

We have investigated the possibility of superconductivity in the electron gas by employing the method of effective-potential expansion. Superconductivity appears when r_s is larger than the critical value $r_{sc}=3.9$. With the increase of r_s, estimated T_c shows a maximum at $r_s=7.2$. The peak value $T_c^{\max}$ divided by $m^*/(m_e\epsilon_0^2)$ is 58 K. The plasmon in the sense of the RPA is important to overcome the bare repulsive Coulomb potential, but the effects beyond the RPA, like the paramagnon-mediated potential, are essential to bring about such a strong instability for superconductivity. In particular, the enhancement of the polarization induced by the local multiple scatterings between the virtually excited electron-hole pair is the most important process. Without these effects beyond the RPA, r_{sc} becomes larger than 20 and $T_c^{\max}/[m^*/(m_e\epsilon_0^2)]$ is of the order of 1 K.

In order to estimate how accurate the present calculations are, we have compared the results for ϵ_c and μ_c with those in the GFMC and found that the relative error is less than 10% for $1\leq r_s\leq 10$. This indicates that the kernel K has an error of the same magnitude. Roughly speaking, T_c is proportional to $\exp(-1/K)$. Thus, near the critical value r_{sc} in which T_c is very small, even a small change of K may produce a very large change in T_c, i.e., a change of more than several orders of magnitude. Therefore, r_{sc} may not be reliable. On the other hand, $T_c^{\max}$ will have a relatively small error. Even if we change K by 10% artificially, the change in $T_c^{\max}$ is less than the factor of 10. We have also checked the errors in r_{sc} and $T_c^{\max}$ by changing the parameters q_c and $\langle k\rangle$ in our theory. We have found that r_{sc} may be as large as 6 and that $T_c^{\max}/[m^*/(m_e\epsilon_0^2)]$ may be in the range 1–10 K.

Let us consider the application of the present results to real materials. Since almost all metals have the r_s value between 2 and 3,[34] there are only a few systems to consider. The first one is the alkali metals Na, K, Rb, and Cs. It is experimentally known that these alkali metals do not show superconductivity at least for $T>1$ mK. Discrepancy between experiment and the present

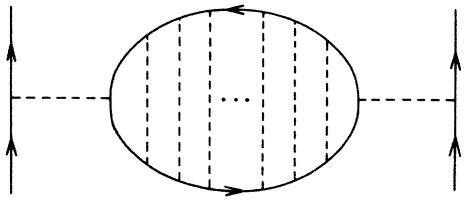

FIG. 20. Diagrammatic representation for the most important process involved in $V_p^{(2e:1)*}$ defined in Eq. (5.22).

theory may be explained in various ways. Firstly, a model of the electron gas may not be suitable for superconductivity in these alkali metals in the following two respects. (1) There are always phonons in the system. These phonons may work destructively when they are included together with the Coulomb interaction in the system. (2) In our theory, the effects beyond the RPA are important to bring about superconductivity for $r_s < 20$, but all these effects are very local in nature. Thus the model of a uniform positive background may give a very different answer from the real situation in which ions should be treated as point charges. Secondly, these metals may already be in other ordered states like the charge-density-wave or the spin-density-wave state,[35] which usually suppress the occurrence of superconductivity. Thirdly, r_{sc} may be larger than 5.62 which is the r_s value for C_s. Lastly, although the conventional values for r_s are determined with the choice of $m^*=m_e$ and $\epsilon_0=1$, ϵ_0 may be larger than unity so that the actual r_s value may be smaller than 3.9 even for C_s.

The second system which we must pay attention to is the recent high-T_c oxide superconductors.[23] Although the r_s value for these materials is not yet known, it is probably correct that r_s is larger than r_{sc}. At the present, it is a general trend to emphasize the one- or two-dimensional behavior of the electrons in the system. However, to have real superconducting transition without fluctuations, we have to consider the system in three dimensions. Thus there is a reason to regard these oxides as an anisotropic three-dimensional electron gas. Since the transfer integral along the c axis is small, m^* estimated by a geometrical average over the a, b, and c axes will be much larger than m_e. In addition, ϵ_0 will be of the order of unity, because no ferroelectric transition has been reported, in contrast to the case of $SrTiO_3$ (Ref. 29) in which ϵ_0 is as large as 10^4. From these considerations we expect that the factor $m^*/(m_e\epsilon_0^2)$ is of the order of unity; thus T_c is in the range 10–100 K.

Admittedly, to regard these oxides as an electron gas will be too simple to explain all the details of experiments. However, we cannot find any apparent inconsistency between our viewpoint and experiments. On the contrary, there are several experiments which are consistent with our viewpoint. The details of the discussion have already been published.[22]

There are two difficult problems which are left for the future. First, we have to develop a finite-temperature version of the present theory to discuss physical properties like the ratio Δ_k at $T=0$ to k_BT_c. We anticipate that Eq. (1.6) will be derived by a finite-temperature formalism, but the dependence of $\tilde{\epsilon}_k$ on temperature might be important, especially for the case in which $\tilde{\epsilon}_k$ becomes positive for k in the range from $0.96k_F$ to k_F, as in Fig. 14(b). Since $\tilde{\epsilon}_k$ in this region has the magnitude of order k_BT_c, these positive region of $\tilde{\epsilon}_k$ may vanish for $T=T_c$, so that $\tilde{\epsilon}_k$ may be very close to the bare one $\epsilon_k-\mu_H$. When we used $\epsilon_k-\mu_H$ in Eq. (1.6) instead of $\tilde{\epsilon}_k$, we obtained a lower T_c as shown in Fig. 18(b). Therefore, the ratio $2\Delta_{k_F}/k_BT_c$ might be larger than the BCS value, 3.52.

Another problem is to include phonons into the system. This is quite important in order to discuss the effect of Coulomb interaction on superconductivity in ordinary metals. It may be incorrect to assume that the effect of Coulomb potential can be treated separately from that of the phonon-mediated potential. However, if we assume it, the present result indicates that the Coulomb pseudopotential μ^* becomes negative in relatively low-carrier-density systems, in contrast with a naive belief that μ^* will become larger than 0.1. One important consequence from the possibility of negative μ^* is that the strong-coupling limit of Allen and Dynes[16] can be reached rather easily. According to Cai *et al.*,[36] T_c is proportional to $[\lambda/(1+2.60\mu^*)]^{1/2}$ when the electron-phonon coupling constant λ is large. This indicates that we will obtain the same value for $\lambda/(1+2.60\mu^*)$ with $\lambda=1$ and $\mu^*=-0.25$ as with $\lambda=3.6$ and $\mu^*=0.1$. The negative μ^* also paves the way to explain the observed T_c and the isotope-effect coefficient α simultaneously in the recent oxide superconductors without resorting to the use of unreasonably large values of λ.[37]

[1]See, for example, D. Rainer, in *Progress in Low Temperature Physics,* edited by D. F. Brewer (North-Holland, Amsterdam, 1986), Vol. 10, p. 371.

[2]N. N. Bogoliubov, V. V. Tolmachev, and D. V. Shirkov, *New Method in the Theory of Superconductivity* (Consultants Bureau, New York, 1959); P. Morel and P. W. Anderson, Phys. Rev. **125**, 1263 (1962).

[3]See, for example, G. R. Stewart, Rev. Mod. Phys. **56**, 755 (1984).

[4]Y. Takada, J. Phys. Soc. Jpn. **45**, 786 (1978).

[5]D. A. Kirzhnits, E. G. Maksimov, and D. I. Khomskii, J. Low Temp. Phys. **10**, 79 (1973).

[6]H. Rietschel and L. J. Sham, Phys. Rev. B **28**, 5100 (1983).

[7]G. H. Eliashberg, Zh. Eksp. Theor. Fiz. **38**, 966 (1960) [Sov. Phys.—JETP **11**, 696 (1960)].

[8]M. Grabowski and L. J. Sham, Phys. Rev. B **29**, 6132 (1984).

[9]F. Coester and H. Kümmel, Nucl. Phys. **17**, 477 (1960).

[10]T. Morita, Prog. Theor. Phys. **20**, 920 (1958); J. M. J. van Leeuwen, J. Groeneveld, and J. de Boer, Physica (Utrecht) **25**, 792 (1959); E. Krotscheck and M. L. Ristig, Phys. Lett. **48A**, 17 (1974); Nucl. Phys. **A242**, 389 (1975); S. Fantoni and S. Rosati, Lett. Nuovo Cimento **10**, 545 (1974); Nuovo Cimento **25A**, 593 (1975).

[11]R. F. Bishop and K. H. Lührmann, Phys. Rev. B **26**, 5523 (1982).

[12]K. Emrich and J. G. Zabolitzky, Phys. Rev. B **30**, 2049 (1984).

[13]L. J. Lantto, Phys. Rev. B **22**, 1380 (1980); J. G. Zabolitzky, *ibid.* **22**, 2353 (1980).

[14]E. Krotscheck, R. A. Smith, A. D. Jackson, Phys. Rev. B **24**, 6404 (1981); S. Fantoni, in *Recent Progress in Many-Body Theories,* Vol. 142 of *Lecture Notes in Physics,* edited by J. G.

Zabolitzky, M. de Llano, M. Fortes, and J. W. Clark (Springer, New York, 1981), p. 129; K. Emrich, *ibid.*, p. 121; K. Emrich and J. G. Zabolitzky, in *Recent Progress in Many-Body Theories,* Vol. 198 of *Lecture Notes in Physics,* edited by H. Kümmel and M. L. Ristig (Springer, Berlin, 1984), p. 271.

[15]D. J. Scalapino, J. R. Schrieffer, and J. W. Wilkins, Phys. Rev. **148**, 263 (1966); W. L. McMillan, *ibid.* **167**, 331 (1968); D. J. Scalapino, in *Superconductivity,* edited by R. D. Parks (Dekker, New York, 1969), Vol. 1, p. 449.

[16]P. B. Allen and R. C. Dynes, Phys. Rev. B **12**, 905 (1975); P. B. Allen and B. Mitrović, in *Solid State Physics,* edited by H. Ehrenreich, F. Seitz, and D. Turnbull (Academic, New York, 1982), Vol. 37, p. 1.

[17]Y. Takada, Phys. Rev. A **28**, 2417 (1983).

[18]Y. Takada, Phys. Rev. B **30**, 3882 (1984).

[19]D. M. Ceperley and B. J. Alder, Phys. Rev. Lett. **45**, 566 (1980); S. H. Vosko, L. Wilk, and M. Nusair, Can. J. Phys. **58**, 1200 (1980).

[20]Y. Takada, Phys. Rev. B **35**, 6923 (1987).

[21]J. Bardeen, L. N. Cooper, and J. R. Schrieffer, Phys. Rev. **108**, 1175 (1957).

[22]Very preliminary results were reported by Y. Takada, in *Novel Superconductivity,* edited by S. A. Wolf and V. Z. Kresin (Plenum, New York, 1987), p. 435. A minor numerical error was involved in the result for μ_c, but it has been corrected in the present paper.

[23]J. B. Bednorz and K. A. Mueller, Z. Phys. B **64**, 189 (1986); M. K. Wu, J. R. Ashburn, C. J. Torng, P. H. Meng, L. Gao, Z. J. Huang, Y. Q. Wang, and C. W. Chu, Phys. Rev. Lett. **58**, 908 (1987); See also, for example, Phys. Today **40(4)**, 17 (1987).

[24]N. N. Bogoliubov. Zh. Eksp. Teor. Fiz. **34**, 58 (1958) [Sov. Phys.—JETP **7**, 41 (1958)]; J. G. Valatin, Nuovo Cimento **7**, 843 (1958).

[25]M. Gell-Mann and K. Brueckner, Phys. Rev. **106**, 364 (1957).

[26]J. Hubbard, Proc. R. Soc. London, Ser. A **243**, 336 (1957).

[27]T. M. Rice, Ann. Phys. (N.Y.) **31**, 100 (1965).

[28]L. Hedin, Phys. Rev. **139**, A796 (1965).

[29]Y. Takada, J. Phys. Soc. Jpn. **49**, 1267 (1980).

[30]F. S. Khan and P. B. Allen, Solid State Commun. **36**, 481 (1980).

[31]B. Schuh and L. J. Sham. J. Low Temp. Phys., **50**, 391 (1983).

[32]P. Hohenberg and W. Kohn, Phys. Rev. **136**, B864 (1964).

[33]W. Kohn and L. J. Sham, Phys. Rev. **140**, A1133 (1965).

[34]See, for example, N. W. Ashcroft and N. D. Mermin, *Solid State Physics* (Saunders College, Philadelphia, 1976), p. 5.

[35]W. A. Overhauser, Phys. Rev. Lett. **4**, 462 (1960); Phys. Rev. **128**, 1437 (1962); **167**, 691 (1968); Adv. Phys. **27**, 343 (1978); T. M. Giebultowicz, A. W. Overhauser, and S. A. Werner, Phys. Rev. Lett. **56**, 1485 (1986); **56**, 2228 (1986).

[36]J. Cai, G. Ji, H. Wu, J. Cai, and C. Gong, Scí. Sin. **22**, 417 (1979).

[37]Y. Takada, Physica (to be published).